Mottl, M.J., Davis, E.E., Fisher, A.T., and Slack, J.F. (Eds.), 1994
Proceedings of the Ocean Drilling Program, Scientific Results, Vol. 139

5. LATE QUATERNARY CALCAREOUS NANNOFOSSILS FROM THE SEDIMENTED MIDDLE VALLEY OF THE JUAN DE FUCA RIDGE, LEG 139[1]

Shaozhi Mao[2,3] and Sherwood W. Wise, Jr.[2]

ABSTRACT

Upper Quaternary calcareous nannofossils contained in drill cores taken in the heavily sedimented Middle Valley of the northern Juan de Fuca Ridge in the northeast Pacific Ocean (Ocean Drilling Program Leg 139) are investigated. The host sediments have been subjected at depth to high temperatures and hot hydrothermal fluids that have altered or destroyed in part or in toto the nannofossil assemblages, thereby raising at several sites the level of the first (deepest) stratigraphic occurrence of nannofossils or of the important *Emiliania huxleyi* datum. The degree of alteration of the nannofossil assemblages is dependent on the intensity of the hydrothermal activity, which is indicated by paleotemperatures derived independently from studies of color alteration of palynomorphs and by vitrinite reflectance (Mao et al., this volume). State of preservation and the downhole level at which assemblages have been destroyed correlate well with the inferred paleotemperature estimates. Destruction of the assemblages appears to be species selective and follows in general the dissolution rankings determined independently by others for Recent nannofossils of the Pacific basin. More systematic correlation of these phenomena is hampered, however, by the fact that nannofossil preservation is already quite variable at the time of deposition because of the predominance of turbidite activity in the study area.

INTRODUCTION

During Leg 139 of the Ocean Drilling Program (ODP), *JOIDES Resolution* drilled Middle Valley of the northern Juan de Fuca Ridge (northeast Pacific Ocean). This was the first part of a proposed two-leg program to investigate hydrothermal processes and products along a sedimented ocean ridge. Although magma is supplied in abundance along most of the Juan de Fuca Ridge, in the drilling area (a deep extensional rift filled with thick Pleistocene sediments), the magma supply is significantly diminished. However, hot hydrothermal fluids from the underlying igneous basement have interacted with the sediments. Twenty-two holes at four sites (Fig. 1; Table 1) were drilled in the valley, where the sediments are mainly hemipelagic clays and turbidite sequences. The purpose of this paper is to describe the calcareous nannofossils from this unusual geological setting and to assess the effects of the hydrothermal fluids on the fossil assemblages.

We are aware of no previous studies of nannofossil assemblages that have been subjected to hydrothermal activity. However, the intrusion of high-temperature hydrothermal solutions containing dissolved chemical compounds and gas (such as CO_2) should result in the destruction of nannofossil ultrastructures and/or the partial or total dissolution of the nannofossil assemblages. Similarly, high heat flow would raise in-situ pore fluid temperatures, thereby increasing reaction rates and promoting the dissolution of nannofossils. Consequently, where strong hydrothermal activity has occurred, one might expect poor preservation, with any assemblages recorded representing only the distorted remnants of the original material. In addition, the first (deepest) stratigraphic occurrences of some key taxa may be found higher in the section than expected, a circumstance that would hamper the development of a precise biostratigraphy.

The specific goals of this paper are to establish the calcareous nannofossil stratigraphy as precisely as possible, to estimate sedimentation rates where feasible, and to survey the diagenetic effects of hydrothermal activity on nannofossil assemblages. In particular, we will explore the relationship between nannofossil preservation and hydrothermal temperature.

Four hundred and ninety-seven samples from 12 holes at four sites were examined. One hundred ninety-one samples are barren of nannofossils, accounting for 38.5% of the total (Table 2). Among the 306 fossiliferous samples, 44 contain rare and poorly preserved specimens of a single species, *Coccolithus pelagicus*.

MATERIALS AND METHODS

Smear slides were prepared directly from the raw sediment samples and were investigated by conventional light microscopy. For scanning electron microscope (SEM) studies, the raw sediments were disaggregated and settled to remove coarse particles and to concentrate the fossils.

The distribution, preservation, and abundance of nannofossils for each hole are presented in range charts (Tables 3–10). Because calcareous nannofossils in the study area constitute only a small portion of the sediment, the relative abundance of individual species and assemblages were estimated as follows (at a magnification of 1560×):

A = abundant, >10–100 specimens/field of view;
C = common, 1–10 specimens/field;
F = few, 1 specimen/2–10 fields;
R = rare, 1 specimen/11–100 fields;
B = essentially barren, 1 specimen/>100 fields.

Qualitative descriptions of nannofossil preservation in each sample were recorded as follows:

M = moderate, significant evidence of secondary alteration via etching and/or destruction of some elements; identification of species generally not impaired.

P = poor, specimens with severe etching and destruction of some elements; identification of some species significantly impaired.

VP = very poor, specimens strongly altered, showing rough outlines with structures heavily damaged due to hydrothermal alteration.

For each sample at least 100 fields were scanned. The biostratigraphic zonation employed here is that of Martini (1971). Additional zonal markers suggested by Gartner (1977), Gard (1988), Verbeek (1990), Rio et al. (1990), and Sato et al. (1991) were also used wherever

[1] Mottl, M.J., Davis, E.E., Fisher, A.T., and Slack, J.F. (Eds.), 1994. *Proc. ODP, Sci. Results*, 139: College Station, TX (Ocean Drilling Program).
[2] Department of Geology, Florida State University, Tallahassee, Florida 32306, U.S.A.
[3] Present address: Department of Geology, China University of Geosciences, Xueyan Road 29, 100083, Beijing, People's Republic of China.

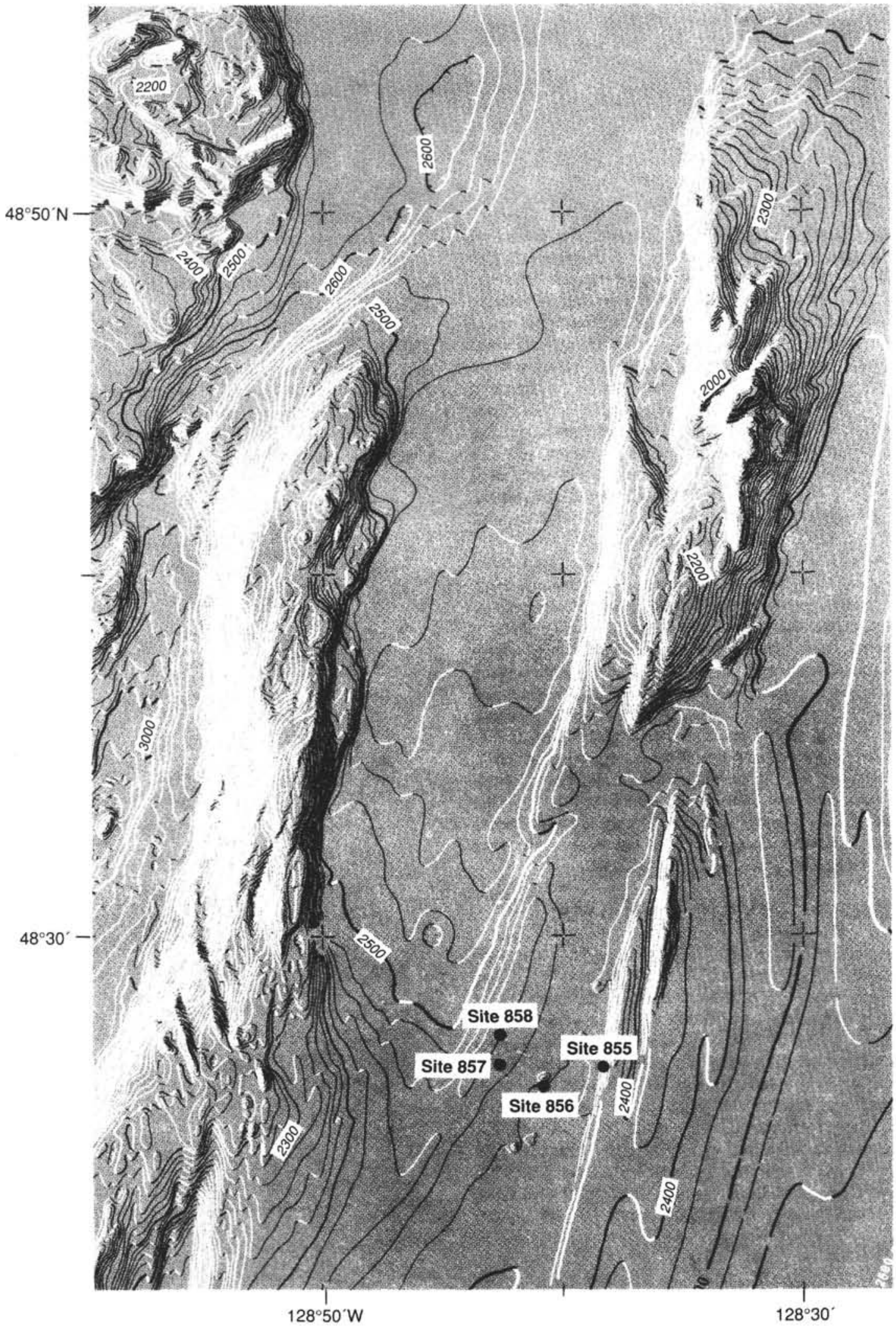

Figure 1. Location map of study area.

Table 1. Water depth and location of Leg 139 sites.

Site	Latitude and longitude	Water depth (m)
855	48° 26.56′ N 128° 38.27′ W	2456
856	48° 26.20′ N 128° 40.84′ W	2406
857	48° 26.5′ N 128° 42.6′ W	2433
858	48° 27.34′ N 128° 42.54′ W	2420

possible, particularly the *Emiliania huxleyi* acme of Gartner (1977). Most of the zonal markers have previously been correlated with the geomagnetic-reversal time scale of Berggren et al. (1985).

BIOSTRATIGRAPHIC AND TAXONOMIC CONCEPTS

During the past fifteen years Quaternary nannofossil biostratigraphy has been intensively studied in an attempt to improve precision for climate-change studies. Gartner (1977) proposed seven biozones for this time interval. Others have tried quantitative or semiquantitative methods to divide some genera into different morpho-groups (rather than species) that could be related to biostratigraphic zones (Matsuoka and Okada, 1989; Gard, 1988; Gard and Backman, 1990). For example, Gard (1988) subdivided four late Quaternary zones of Gartner (1977) into 11 zones based on the study of *Gephyrocapsa.*

In the study area, because of the hydrothermal activity and the dominantly turbiditic sedimentation, the nannofossil assemblages extracted from the sediments may represent the final products of gravity sorting, mechanical erosion, and hydrothermal alteration. This makes it difficult to establish a detailed stratigraphic subdivision such as those of Gard (1988) and Matsuoka and Okada (1989). However, we found that the standard zonation schemes and many of the new biostratigraphic datums proposed by the authors mentioned above are still useful for this study.

In general, nannofossil assemblages in the study area are of low diversity, ranging from only one to about 20 taxa, with *Gephyrocapsa* spp., *Emiliania huxleyi,* and *Coccolithus pelagicus* the most dominant. *Gephyrocapsa* species are difficult to distinguish with both the light microscope (LM) and the SEM (Perch-Nielsen, 1985). The taxonomy of the genus is ambiguous and controversial, with many forms difficult to differentiate at the species level. Matsuoka and Okada (1990) roughly divided *Gephyrocapsa* into two categories, small (specimens ~2.0–3.5 µm) and large (specimens >3.5 µm). The small category may consist of several species such as *G. aperta, G. ericsonia, G. pelta,* and *G. sinuosa.* For the large forms, these authors noticed time-progressive changes in overall size and bridge angle and identified with the aid of statistics four groups (A, B, C, and D). Each of these four groups has a different stratigraphic range.

Gard (1988) also observed during her study of European Arctic seas that *Gephyrocapsa* spp. showed characteristic morphological changes through time. Three basic morphotypes of *Gephyrocapsa* were easily recognized under the light microscope as follows: (1) slightly ovoid specimens about 2.5–5 µm in length with a bridge spanning an open central area (described variously as *G. muellerae* Bréhérét or *G. oceanica* Kamptner, and referred to as *G. muellerae* by Gard); (2) distinctly small specimens, <2.5 µm, usually only about 1 µm in length (described variously as *G. aperta* Kamptner, *G. ericsonii* McIntyre and Bé, and/or *G. theyerii* Pujos, and referred to as *G. aperta* by Gard); (3) Specimens 2.5–5 µm in diameter with closed or nearly closed central area spanned by a short and not clearly visible bridge under the light microscope (referred to as *G. carribeanica* Boudreaux and Hay by Gard).

Table 2. Numbers of samples examined and percentage of fossiliferous samples in each hole.

Holes	Total samples	Fossiliferous samples	% of total
855A	24	24	100
855B	8	7	87.5
855C	44	39	88.5
855D	1	0	0
856A	67	31	46
856B	53	1	2
857A	95	89	93.5
857C	99	51	51.5
858A	60	40	65.5
858B	10	5	50
858C	13	8	61.5
858D	23	11	48
Total	497	306	61.5

In their study of calcareous nannofossils from the western Mediterranean, Rio et al. (1990) stated that the overall size of gephyrocapsids does indeed represent a plain morphometric parameter and can be used to consistently correlate lower Pleistocene sequences from geographically distant areas. They split the group into four categories as follows: (1) specimens <3.5 µm in size, labeled "small *Gephyrocapsa* spp."; (2) specimens >4 µm and <5.5 µm in size with a central opening, labeled *G. oceanica* s.l.; (3) specimens >5.5 µm, labeled "large *Gephyrocapsa* spp."; (4) specimens usually 4–6 µm in size with an open central area and a bridge nearly aligned with the short axis of the placolith (labeled *Gephyrocapsa* sp. 3 by Rio, 1982), comparable to *G. parallela* of Takayama and Sato (1987) or *G. omega* Bukry of most other authors.

Gard's classification of *Gephyrocapsa* is employed as the basic scheme for this study in view of the state of preservation and the geographic proximity of the study area to the subarctic area. The other schemes are also referenced. We divide *Gyphyrocapsa* into four groups by splitting Group 1 of Gard into two groups. Our Group 1 is equal to the smaller size (~2.5–3.5 µm) fraction of Gard's Group 1 while our Group 4 is equal to the larger size (>3.5–5 µm). Our Groups 2 and 3 are the same as those of Gard. Therefore, our Group 4 corresponds to *Gephyrocapsa* sp. D of Matsuoka and Okada (1989) or *Gephyrocapsa oceanica* of most authors.

RESULTS

Site 855

Four holes were drilled at Site 855 (water depth = 2456 m) along a normal fault that forms the eastern topographic boundary of the sedimented rift valley; all recovered upper Pleistocene sediments. Three holes produced the most fossiliferous samples of all the drill sites; however, the species diversity is as low as at the other three sites, consisting of only 1 to 16 taxa (Tables 3–5).

The marker species, *Emiliania huxleyi,* is common in samples above 14.58 mbsf at Hole 855A and above 17.04 mbsf at Hole 855C, but is few to rare in samples below these depths; it never is abundant in any holes of this site. According to Perch-Nielsen (1985) this species presently exhibits its widest distribution. It is found in high latitudes as well as in the tropics. It also is one of the last species to be dissolved when sinking to great ocean depths (Schneidermann, 1977). However, it is so delicate in structure, with many isolated "T"-shaped elements along the distal shield, that heat flow and hydrothermal fluids may destroy it partially or completely. As a result, the numbers of *E. huxleyi* in nannofossil assemblages may be reduced or altered. At Site 855 the first occurrence of *E. huxleyi* is difficult to detect because of its low

Table 3. Distribution of calcareous nannofossils, Hole 855A, Leg 139.

Lithologic unit	Hole 855A Core, section interval (cm)	Depth (mbsf)	Abundance	Preservation	*Braarudosphaera bigelowii*	*Calcidiscus leptoporus*	*Coccolithus crassipons*	*Coccolithus pelagicus*	*Coccolithus streckerii*	*Crenalithus doronicoides*	*Emiliania huxleyi*	*Emiliania pujosae*	*Gephyrocapsa* Group 1	*Gephyrocapsa* Group 2	*Gephyrocapsa* Group 3	*Gephyrocapsa* Group 4	*Helicosphaera kampineri*	*Helicosphaera wallichii*	*Pontosphaera japonica*	*Pontosphaera* sp.	Zonation (Martini, 1971)	Age (Based on data from forams and nannos)
II	1R-1, 91-94	0.91	A	M	.	.	.	R	.	F	C	.	C	.	.	.	.	.	.	.	NN21 *Emiliania huxleyi* Acme	Holocene
II	1R-2, 88-90	2.38	A	M	F	.	.	C	.	.	C	.	A	.	.	C	.	.	R	.	NN21 *Emiliania huxleyi* Acme	Holocene
II	1R-3, 91-94	3.91	C	M	R	.	.	C	.	.	F	R	C	.	.	F	.	.	.	R	NN21 *Emiliania huxleyi* Acme	Holocene
II	1R-4, 94-97	5.44	A	M	F	.	R	A	F	F	C	C	A	R	.	.	.	.	.	F	NN21 *Emiliania huxleyi* Acme	Holocene
II	1R-5, 80-82	6.80	A	M	.	.	.	C	.	F	C	.	C	.	.	.	.	.	.	.	NN21 *Emiliania huxleyi* Acme	Holocene
II	2R-1, 99-101	8.59	F	P	.	.	.	F	.	.	C	F	C	R	.	.	.	.	.	.	NN21 *Emiliania huxleyi* Acme	late Pleistocene
II	2R-2, 99-101	10.09	C	P	.	.	.	C	.	.	C	.	C	.	.	.	.	.	.	F	NN21 *Emiliania huxleyi* Acme	late Pleistocene
II	2R-3, 99-101	11.59	C	M	.	R	.	C	R	.	C	.	C	F	.	.	.	.	.	.	NN21 *Emiliania huxleyi* Acme	late Pleistocene
II	2R-4, 100-102	13.11	F	P	.	.	.	F	.	R	F	.	F	R	R	.	.	.	.	.	NN21 *Emiliania huxleyi* Acme	late Pleistocene
II	2R-5, 98-102	14.58	A	P	R	R	.	C	.	.	F	.	C	F	.	.	.	.	.	.	NN21 *Emiliania huxleyi* Acme	late Pleistocene
II	3R-1, 19-21	16.79	C	P	R	R	R	C	.	.	.	.	C	F	.	R	.	.	.	F	NN21	late Pleistocene
II	3R-2, 19-21	18.29	F	P	.	.	.	F	.	.	R	.	F	.	.	.	.	.	.	.	NN21	late Pleistocene
II	3R-3, 23-25	19.83	F	P	.	.	.	F	.	.	R	.	F	.	.	.	.	.	.	.	NN21	late Pleistocene
II	4R-1, 19-21	26.19	C	P	.	.	.	F	.	.	R	.	C	F	.	.	.	.	.	.	NN21	late Pleistocene
II	4R-2, 20-22	27.70	C	P	.	.	.	C	.	.	R	.	F	.	.	.	.	.	.	R	NN21	late Pleistocene
II	4R-3, 22-24	29.22	A	P	.	.	R	C	.	C	R	.	A	C	F	.	.	.	.	R	NN21	late Pleistocene
II	4R-4, 48-50	30.98	F	P	.	.	.	C	.	.	R	.	F	.	.	.	.	.	.	R	NN21	late Pleistocene
II	5R-1, 13-15	35.63	C	P	.	.	.	F	.	R	F	.	C	F	.	.	.	.	.	.	NN21	late Pleistocene
II	6R-1, 91-94	46.41	C	P	.	.	.	F	.	.	R	.	C	F	.	.	.	.	.	.	NN21	late Pleistocene
II	6R-2, 0-4	47.00	C	M	.	.	.	F	.	.	R	.	C	R	.	R	.	.	.	.	NN21	late Pleistocene
II	7R-1, 92-96	56.02	R	P	.	.	.	.	.	.	.	.	R	.	.	.	.	.	.	.	NN21	late Pleistocene
II	7R-2, 72-76	57.32	A	P	.	.	.	C	.	F	.	.	A	F	.	.	.	.	.	.	NN21	late Pleistocene
II	7R-3, 18-22	58.28	A	M	.	F	R	C	.	F	R	.	A	F	F	.	R	R	R	.	NN21	late Pleistocene

Table 4. Distribution of calcareous nannofossils, Hole 855B, Leg 139.

Lithologic unit	Hole 855B Core, section interval (cm)	Depth (mbsf)	Abundance	Preservation	*Braarudosphaera bigelowii*	*Coccolithus pelagicus*	*Crenalithus doronicoides*	*Emiliania huxleyi*	*Emiliania pujosae*	*Gephyrocapsa* Group 1	*Gephyrocapsa* Group 2	*Gephyrocapsa* Group 3	*Gephyrocapsa* Group 4	*Syracosphaera* sp.	Zonation (Martini, 1971)	Age (Based on data from forams and nannos)
I	2R-1, 94-98	6.64	A	P	R	C	F	R	.	A	.	.	R	R	NN21	late Pleistocene
I	2R-2, 64-68	7.84	A	M	.	C	R	R	.	C	C	.	.	.	NN21	late Pleistocene
I	4R-1, 51-55	25.01	C	P	.	F	.	R	.	C	.	.	.	.	NN21	late Pleistocene
I	4R-2, 51-55	26.51	R	P	.	R	.	R	.	R	.	.	.	.	NN21	late Pleistocene
I	4R-4, 51-55	28.01	R	P	.	R	.	R	.	R	.	.	.	.	NN21	late Pleistocene
I	4R-5, 51-55	30.01	F	P	.	F	.	R	R	F	.	.	.	.	NN21	late Pleistocene
I	5R-1, 34-40	34.34	C	P	.	F	F	R	.	C	R	F	F	.	NN21	late Pleistocene

abundance (1 specimen/more than 50 fields in Sample 139-855A-9R-CC). This species is rare in all seven samples from Hole 855B. In Hole 855C *E. huxleyi* is rare in most samples below Sample 139-855C-2R-6, 84–88 cm, and disappears from samples below Core 139-855C-10R. In general, most of the section in Hole 855C and the whole section in Holes 855A and 855B can be assigned to the nannofossil *E. huxleyi* Zone (NN21) of Martini (1971). The absence of *E. huxleyi* in Hole 855C from the bottom of Core 139-855C-11R may be the result of poor preservation.

Gartner (1977) defined the *E. huxleyi* Acme Zone by the dominance of *E. huxleyi* over the assemblage, suggesting that *E. huxleyi* is the most abundant species from this zone. Gard (1988) defined her Zone N-G1 as the interval from the Recent down to the point that *Coccolithus pelagicus* dramatically decreases in total abundance. *Coc-*

Table 5. Distribution of calcareous nannofossils, Hole 855C, Leg 139.

Lithologic unit	Hole 855C Core, section interval (cm)	Depth (mbsf)	Abundance	Preservation	*Braarudosphaera bigelowii*	*Calcidiscus leptoporus*	*Coccolithus crassipons*	*Coccolithus pelagicus*	*Coccolithus streckerii*	*Crenalithus doronicoides*	*Emiliania huxleyi*	*Emiliania pujosae*	*Gephyrocapsa* Group 1	*Gephyrocapsa* Group 2	*Gephyrocapsa* Group 3	*Gephyrocapsa* Group 4	*Pontosphaera japonica*	*Pontosphaera* sp.	*Reticulofenestra* sp.	*Syracosphaera pulchra*	Zonation (Martini, 1971)	Age (Based on data from forams and nannos)
I	1R-1, 92-96	0.92	C	G	R	F	.	C	.	R	C	F	C	F	.	F	.	.	.	.	NN21 (*Emiliania huxleyi* Acme)	Holocene
	1R-2, 94-96	2.44	A	M	R	.	.	C	R	F	C	R	C	R	.	F	R	.	.	.		
	1R-3, 110-112	4.10	A	M	R	.	R	C	.	.	C	F	C	.	.	F	.	.	.	.		
	1R-4, 95-97	5.45	A	M	R	.	.	C	R	.	C	F	C	.	.	.	.	.	.	R		
	1R-6, 47-49	7.79	C	M	R	.	.	C	.	.	C	F	C	R	.	R	.	.	.	.		
	2R-1, 114-118	9.84	A	M	F	.	.	C	R	.	C	F	C	F	.	R	.	.	.	.		late Pleistocene
	2R-2, 91-95	12.56	A	M	F	R	.	C	.	.	C	F	A	R	.	.	.	.	.	.		
	2R-3, 86-92	13.53	C	P	.	R	.	F	.	.	C	F	C	.	R	R	.	.	.	.		
	2R-4, 33-37	11.11	C	P	.	R	.	F	.	.	C	F	C	.	.	.	.	.	.	.		
	2R-5, 95-99	15.65	F	M	.	.	.	R	.	.	F	R	R	.	.	.	.	.	.	.		
	2R-6, 84-88	17.04	C	M	.	R	.	F	.	.	C	F	C	F	.	.	.	.	.	.		
	3R-1, 90-92	21.67	R	P	.	.	.	R	.	.	.	.	R	.	.	.	.	.	.	.	NN21	
	3R-2, 53-55	18.60	R	P	.	.	.	R	.	.	.	.	.	.	.	.	.	.	.	.		
	3R-3, 97-99	19.73	R	M	.	.	.	R	.	.	R	.	R	.	.	.	.	.	.	.		
	3R-4, 56-58	22.76	R	P	.	.	.	R	.	.	R	.	R	.	.	.	.	.	.	.		
	4R-1, 42-44	29.01	R	P	.	.	.	.	.	.	R	.	R	.	.	.	.	.	.	.		
	4-R2, 41-43	27.52	F	M	.	.	.	F	.	.	F	.	F	.	.	.	.	.	.	.		
	4R-3, 62-64	30.72	F	M	R	.	.	F	.	.	F	.	R	F	.	.	.	.	.	.		
	4R-4, 17-19	31.72	C	M	R	.	.	C	.	.	F	.	F	F	.	.	.	.	.	R		
	4R-5, 51-55	31.77	R	P	.	.	.	R	.	.	R	.	R	.	.	.	.	.	.	.		
	6R-1, 6-10	46.56	F	P	.	.	R	F	.	.	R	.	F	R	.	.	.	.	.	.		
	6R-2, 12-16	48.12	F	P	R	.	.	F	.	R	R	.	F	.	R	F	.	.	.	.		
	6R-3, 6-10	52.58	C	P	.	.	.	F	.	.	R	.	C	F	F	F	.	.	.	.		
	6R-4, 10-14	54.02	F	P	R	.	.	F	.	F	R	.	F	F	R	R	.	.	.	.		
	6R-5, 8-12	55.53	C	P	.	.	.	F	.	R	R	.	C	F	R	F	.	.	.	.		
	6R-6, 2-6	49.56	C	M	.	.	.	F	.	.	R	.	C	F	F	F	.	.	.	.		
	6R-7, 3-7	51.10	C	M	.	R	.	F	.	C	R	.	F	.	.	F	.	.	F	.		
	7R-1, 94-98	57.04	C	M	.	.	.	F	.	F	R	.	C	R	.	.	.	.	.	.		
	7R-2, 95-99	64.26	F	P	.	.	.	.	.	R	.	.	F	.	.	.	.	.	.	.		
	7R-3, 107-111	58.55	F	P	.	.	.	.	.	.	.	.	F	.	.	.	.	.	.	.		
	7R-4, 93-97	60.17	A	M	.	.	F	C	.	C	.	.	A	.	C	F	R	F	.	.		
	7R-6, 66-70	85.86	F	P	.	.	.	R	.	.	.	.	F	.	.	.	.	.	.	.		
	9R-1, 44-48	61.53	A	P	.	.	R	C	.	.	.	.	A	C	C	R	.	.	.	.		
	10R-1, 96-100	89.47	A	M	R	R	.	F	.	F	?	.	C	F	C	C	.	.	.	.		
	10R-3, 15-19	74.05	C	P	.	.	.	F	.	F	.	.	C	C	C	F	.	.	.	.		
	10R-4, 13-17	86.55	C	P	.	.	.	F	.	.	.	.	C	F	F	F	.	.	.	.		
	10R-5, 7-11	95.02	C	P	.	.	.	.	.	F	R	.	C	F	.	R	.	.	.	.		
	11R-1, 42-47	88.03	C	P	.	.	.	F	.	F	.	.	C	F	.	.	.	.	.	.		
	11R-2, 24-27	96.34	R	P	.	.	.	R	.	.	.	.	R	.	.	.	.	.	.	.		

colithus pelagicus and *E. huxleyi* dominate the nannofossil assemblages in Zone N-G1, which lies within the *E. huxleyi* Acme Zone of Gartner (1977). Verbeek (1990), however, defined this acme zone (equal to his Zone NAN1) as the interval from the beginning of the acme of *E. huxleyi* to the Present without mentioning whether *E. huxleyi* dominates the nannofossil assemblages or not. In all samples investigated for this work except one (139-858A-2R-5, 6–10 cm), *E. huxleyi* never dominates *Gephyrocapsa* Group 1; instead, the latter is usually the most abundant form, even in the uppermost Holocene sediments. We also noticed that *E. huxleyi* increases its abundance distinctly from few-rare (1 specimen/several to some tens of fields of view) to common (2–9 specimens/field) at about 14–17 mbsf in Holes 855A, 855C, 856A, and 857A. Therefore, we assume the base of the *E. huxleyi* Acme Zone to be at 14.58 mbsf in Hole 855A and at 17.04 mbsf in Hole 855C.

Gephyrocapsa, as mentioned above, is the most abundant taxa and occurs in every sample from this site. *Gephyrocapsa* Group 1 (specimens 2.5–3.5 µm long) dominates the other three groups in Holes 855A, 855B, and 855C. This also supports the conclusions above based on *E. huxleyi* that the whole section from Site 855 can be assigned to Zone NN21 of Martini (1971).

Site 856

Situated over a small hill in the eastern part of Middle Valley (Fig. 1), Site 856 consist of eight holes at a water depth of 2406 m (Table

2). The hill was formed by uplift of the sedimentary section above an intrusion associated with hydrothermal massive sulfide mineralization. Nannofossil investigations could be carried out on only two holes, 856A and 856B. In Hole 856A, more than half of the samples are barren of nannofossils (Table 1 and 6) while in Hole 856B, only one sample contains nannofossils.

The marker species, *E. huxleyi,* is common (2–10 specimens/ field) in samples from Hole 856A above 14.43 mbsf (Sample 139-856A-3H-5, 74–78 cm) except where fossil preservation is poor. This depth (14.43 mbsf) is close to 14.58 mbsf in Hole 855A, which we considered to be the base of the *E. huxleyi* Acme Zone; the same relationship possibly holds for Hole 856A. *Emeliania huxleyi* decreases in number markedly in three samples below 14.43 mbsf and is absent from all samples below 21.54 mbsf (Sample 139-856A-3H-7, 34–38 cm), probably due to the poor preservation caused by hydrothermal activity.

Gephyrocapsa occurs in most samples above Sample 139-856A-6H-2, 59–63 cm (above 41.14 mbsf) and is absent from all samples below this depth.

Gephyrocapsa Group 1 dominates the other three groups of the genus. One specimen of *Helicosphaera inversa* was encountered in Sample 139-856A-3H-5, 74–78 cm. At Site 723 the last appearance datum (LAD) of *H. inversa* is stratigraphically higher than the first appearance datum (FAD) of *E. huxleyi* (Spaulding, 1991). *Coccolithus pelagicus* survived hydrothermal activities to the depth of 51.88 mbsf and is the only species below 41.14 mbsf.

We assume that the section above 14.43 mbsf in Hole 856A as well as Core 139-856B-1H belongs to the *E. huxleyi* Acme Zone. Unfortunately, however, we cannot detect the base of Zone NN21 of Martini (1971) because poor preservation resulted in incomplete fossil records.

Site 857

Site 857, at a water depth of 2433 m (Table 2), is located 1.5 km east of the sediment-buried fault that forms the current structural boundary of the central rift. The site lies over a major thermal anomaly, an area extending 10 km in a rift-parallel direction (Fig. 1). Two km north of the site is a hydrothermal vent field where heat flow exceeds $4 W/m^2$ and fluids discharge at seafloor temperatures up to 276°. Four holes were drilled at this site, reaching the deepest depth in the study area (936 mbsf); however, the nannofossil investigation focused on two holes only, 857A and 857C. Both fossil abundance and species diversity are generally higher in Hole 857A than in Hole 857C (Tables 7 and 8). Despite the deep depth of the latter (519.4 mbsf), nannofossils were encountered mostly above 145.63 mbsf (Sample 139-857C-13R-1, 76–80 cm).

In Hole 857A, *Emiliania huxleyi* was found in most of samples above 73.93 mbsf (Sample 139-857A-9H-4, 3–7 cm) but is common (2–5 specimens/field) only in samples above 17.68 mbsf (Sample 139-857A-2H-5, 28 cm), except where preservation is either poor or general fossil abundance decreases. For the same reason discussed above, we consider this depth (17.68 mbsf) to be the base of the *E. huxleyi* Acme Zone. The first occurrence of *E. huxleyi* in Sample 139-857A-9H-4, 3–7 cm indicates that the section above this point can be assigned to Zone NN21 of Martini (1971). The section below, however, cannot be assigned to any zone due to the lack of marker species, probably due to poor preservation. Group 1 *Gephyrocapsa* in the lower section of Hole 857A, which dominates the other three groups of the genus, supports the conclusion that the whole section of Hole 857A belongs to Zone NN21. The first occurrence of *E. huxleyi* in Hole 857C (Sample 139-857C-12R-2, 63–66 cm) is not entirely reliable because *E. huxleyi* was encountered so rarely (2–3 specimens/100 fields) under the light microscope that it cannot be verified by SEM. *Coccolithus pelagicus* is practically the only species in assemblages from samples immediately below the disappearance of *E. huxleyi;* fossil preservation in these samples is also poor to very poor. Therefore, it is difficult to draw any conclusions on the zonation of the lower 364 m of section at Site 857C.

Site 858

Site 858 lies over an active hydrothermal vent field that extends several hundred meters along and across the strike of Middle Valley (Fig. 1). Heat flow measured in the vent field ranges from $4 W/m^2$ to $20 W/m^2$ (Davis, Mottl, Fisher, et al., 1992). Located 1.8 km north of Site 857, the regional structural setting of Site 858 is similar to that at Site 857. Although seven holes were drilled at this site, sampling for calcareous nannofossils was restricted to four holes (858A, 858B, 858C, and 858D).

Calcareous nannofossils were found only near the top of the section and in less than half of the core sections in these holes; preservation is generally poor to very poor owing to high-temperature hydrothermal diagenesis. As at the other sites, *Gephyrocapsa, Coccolithus pelagicus,* and *Emiliania huxleyi* are the main taxa in most fossiliferous samples, particularly in the former two holes (Tables 9 and 10). The latter usually occurs in the uppermost samples. However, the *E. huxleyi* Acme Zone is difficult to detect, apparently because thermal activity destroyed part or all of the nannofossil assemblages.

Hole 858A has the most abundant and diverse assemblages among the four holes. Fossiliferous samples in this hole reach 81.7 mbsf (Table 9), but only the uppermost section (above 20 mbsf) can be assigned with certainty to Zone NN21 of Martini (1971) based on the occurrence of *E. huxleyi.* Most of the fossiliferous section may still fall within Zone NN21 as suggested by the dominance of *Gephyrocapsa* Group 1. The high heat flow that apparently destroyed the nannofossil assemblages at this site strongly hampered our biostratigraphic studies.

Estimated Sedimentation Rates During the Last 73 k.y.

The *Emiliania huxleyi* Acme Zone was tentatively recognized in Holes 855A (14.58 mbsf), 855C (17.04 mbsf), 856A (14.43 mbsf), and 857A (17.68 mbsf). Sedimentation rates can be obtained based on the chronology of the acme zone (73 k.y. for high latitudes according to Verbeek, 1990). As we calculated for Hole 857A in Davis, Mottl, Fisher, et al. (1992), the sedimentation rates for these holes are as follows:

Hole 855A: 24 cm/ky; Hole 855C: 23 cm/k.y.; and Hole 856A: 23 cm/k.y. Thus, the sedimentation rates in the study area range from 20 cm/k.y. (minimum) to 27 cm/k.y. (maximum).

FOSSIL PRESERVATION/HYDROTHERMAL ALTERATION

McIntyre and McIntyre (1971), Roth and Berger (1975), and Schneidermann (1977) studied the dissolution of Recent calcareous nannofossils in the Indian and Atlantic Oceans. They stated that all coccoliths would be dissolved below the calcium carbonate compensation depth (CCD) and that the skeletal ultrastructure of nannofossils is mainly responsible for the dissolution susceptibility of each species. For example, holococcoliths are readily dissolved while placoliths are highly resistant to solution. Not only is dissolution species selective, but within a single coccolith specimen, selective removal of skeletal elements proceeds in an orderly sequence (Wise, 1977). These conclusions are valid worldwide.

In the study area the water depths of all holes are about 2400–2450 m (Table 2), much shallower than the CCD, which lies at depths of about 4500 m in the equatorial Pacific (Bramlette, 1961) and at about 5500 m in the Atlantic (Turekian, 1965). It seems, therefore, that the poor preservation of calcareous nannofossils in the study area resulted mostly from in-situ hydrothermal activity rather than dissolu-

Table 6. Distribution of calcareous nannofossils, Hole 856A, Leg 139.

(mbsf)	Core	Lithologic unit	Hole 856A Core, section interval (cm)	Depth (mbsf)	Abundance	Preservation	*Braarudosphaera bigelowii*	*Calcidiscus leptoporus*	*Coccolithus crassipons*	*Coccolithus pelagicus*	*Crenalithus doronicoides*	*Emiliania huxleyi*	*Emiliania pujosae*	*Gephyrocapsa* Group 1	*Gephyrocapsa* Group 2	*Gephyrocapsa* Group 3	*Gephyrocapsa* Group 4	*Helicosphaera wallichii*	*Pontosphaera japonica*	*Reticulofenestra* sp.	*Syracosphaera* sp.	*Umbelosphaera tenuis*	Zonation (Martini, 1971)	Age (Based on data from forams and nannos)
0	1	I	1H-1, 137-140	1.37	A	M	.	.	R	C	.	C	F	C	F	.	.	.	.	.	.	.	NN21 *Emiliania huxleyi* Acme	Holocene
			1H-2, 69-72	2.19	C	M	R	.	R	C	.	C	F	C	R	.	.	.	R	.	.	.		late Pleistocene
			2H-1, 52-54	3.22	A	P	R	R	.	F	F	F	.	A	R	.	.	.	.	.	.	.		
	2		2H-2, 50-52	4.70	C	M	.	C	.	F	.	C	.	C	R	.	.	.	.	.	.	.		
			2H-4, 65-67	7.85	C	M	.	F	.	F	.	C	F	C	.	.	.	.	.	.	.	.		
			2H-5, 39-41	9.09	F	P	.	.	.	.	.	R	.	F	.	.	.	.	.	.	.	.		
			3H-1, 103-107	13.23	F	P	.	.	.	F	.	F	.	F	.	.	.	.	.	.	.	.		
			3H-2, 73-77	14.43	C	M	.	F	.	F	F	C	.	C	.	.	.	.	.	.	.	.		
	3		3H-5, 74-78	18.94	C	M	.	F	.	F	.	F	.	F	.	.	F	F	.	.	.	F		
			3H-6, 105-109	20.75	A	M	R	.	.	F	R	F	R	A	C	F	.	R	.	.	R	.		
20			3H-7, 34-38	21.54	C	M	R	.	.	F	R	R	.	C	F	R	.	.	.	.	.	.		
			4H-1, 57-61	22.27	F	P	.	.	.	F	.	.	.	F	R	R	.	.	.	R	.	.	NN21 (?)	late Pleistocene (?)
			4H-2, 72-76	23.92	F	P	R	.	.	F	.	.	.	F	.	R	.	R	.	.	.	.		
	4		4H-3, 25-29	24.95	R	P	.	.	.	R	.	.	.	R	.	.	.	.	.	.	.	.		
		II	4H-4, 28-32	26.48	R	P	R	.	.	R	.	.	.	R	.	.	.	.	.		.	.		
			4H-5, 53-57	28.23	F	P	R	.	.	F	.	.	.	R	.	.	.	.	.	.	.	.		
			4H-6, 45-49	29.65	F	P	R	.	.	F	.	.	.	F	.	.	.	.	.	.	.	.		
			4H-7, 7-11	30.77	R	P	.	.	.	R	.	.	.	R	.	.	.	.	.	.	.	.		
	5		5H-2, 35-39	31.93	C	VP	R	.	.	C	.	.	.	.	.	.	.	.	.	.	.	.		
			5H-3, 38-42	33.46	C	VP	R	.	.	C	.	.	.	.	.	.	.	.	.	.	.	.		
40			5H-4, 37-41	34.95	R	P	.	.	.	R	.	.	.	R	.	R	.	.	.	.	.	.		late Pleistocene
			5H-5, 35-39	36.43	F	P	.	.	.	F	.	.	.	R	.	.	.	.	.	.	.	.		
			5H-6, 35-39	37.93	F	P	.	.	.	F	.	.	.	R	.	.	.	.	.	.	.	.		
	6		5H-7, 33-37	39.41	F	P	.	.	.	F	.	.	.	R	.	.	.	.	.	.	.	.		
			6H-1, 44-48	41.14	F	P	R	.	.	R	.	.	.	F	.	.	.	.	.	.	.	.		
			6H-2, 59-63	42.79	F	VP	.	.	.	F	.	.	.	.	.	.	.	.	.	.	.	.		
			6H-3, 54-58	44.24	F	VP	.	.	.	F	.	.	.	.	.	.	.	.	.	.	.	.		
			6H-4, 55-59	45.75	F	VP	.	.	.	F	.	.	.	.	.	.	.	.	.	.	.	.		
	7		6H-7, 6-10	49.76	R	VP	.	.	.	R	.	.	.	.	.	.	.	.	.	.	.	.		
			7H-1, 52-56	50.72	F	VP	.	.	.	F	.	.	.	.	.	.	.	.	.	.	.	.		
			7H-2, 18-22	54.88	R	VP	.	.	.	R	.	.	.	.	.	.	.	.	.	.	.	.		

tion at depth in the water column. Hydrothermal fluids may contain hot chemical components and gas, which can partially or completely dissolve or destroy fossils and alter the composition of assemblages.

Figure 2 illustrates the lowest sub-bottom depths at which fossiliferous samples and the first occurrences of *Emiliania huxleyi* are found in the different holes. These two depths vary markedly from hole to hole although there is no indication that all biostratigraphic datums vary in a similar fashion. For instance, in Holes 855B, 855C, and 857A, the *E. huxleyi* Acme datum is found at between 15 and 18 mbsf (Fig. 2), but the first occurrence of *E. huxleyi* varies strongly and unpredictably below 21.7 and 101.5 mbsf.

Also plotted against depth in Figure 2 are paleotemperatures inferred from studies of color changes in palynomorphs and from vitrinite reflectance. The depths of these paleotemperature indicators, which increase downhole from <60°C to <200°C, also vary widely from hole to hole. These high-temperature readings are attributed to heat flow associated with hydrothermal activity (Mao et al., this volume).

There is a clear tendency for the first *E. huxleyi* and the first nannofossil datums in Figure 2 to occur at shallower depths in holes where heat flows are or have been high and deeper in holes where heat flows have been low. For example, note the sharp differences between Sites 857 and 858 and between Holes 858A (about 100 m west of the hydrothermal vent field) and 858B (a few meters away from a 276°C hydrothermal vent; Davis, Mottl, Fisher, et al., 1992). The shallow depths of the two nannofossil indicators in question in Hole 856A suggest that the heat flow was about as high there when the vent was active sometime in the past as it is now in Hole 858A even though the measured heat flow from Hole 856A at present is relatively low at only 0.60W/m^2 (Davis, Mottl, Fisher, et al., 1992). This is much lower than that in Hole 858A, and even lower than that in Hole 857A (0.71W/m^2; see Davis, Mottl, Fisher, et al., 1992).

The distance between the first *E. huxleyi* and the first nannofossils should reflect the hydrothermal temperature gradient. The shorter the distance, the steeper the gradient (as in Holes 858B, 858C, and 858D);

Table 7. Distribution of calcareous nannofossils, Hole 857A, Leg 139.

Hole 857A Core, section interval (cm)	Depth (mbsf)	Abundance	Preservation	*Braarudosphaera bigelowi*	*Calcidiscus leptoporus*	*Coccolithus crassipons*	*Coccolithus pelagicus*	*Coccolithus streckerii*	*Crenalithus doronicoides*	*Emiliania huxleyi*	*Emiliania pujosae*	*Gephyrocapsa* Group 1	*Gephyrocapsa* Group 2	*Gephyrocapsa* Group 3	*Gephyrocapsa* Group 4	*Pontosphaera japonica*	*Pontosphaera sp.*	*Reticulofenestra* sp.	*Rhabdoaphaera clavigera*	*Syracosphaera* sp.	*Umbelosphaera tenuis*	Zonation (Martini, 1971)	Age (Based on data from forams and nannos)
1H-1, 28-32	2.18	A	M	R	.	F	C	R	.	C	.	C	F	.	R	F	.	.	.	.	.		Holocene
1H-2, 30-34	3.70	C	M	.	.	F	C	R	.	C	.	C	.	.	R	R	.	.	.	.	.		Holocene
1H-3, 29-33	5.19	A	M	.	.	F	C	R	.	C	F	C	.	.	R	R	.	.	.	.	.		late Pleistocene
1H-4, 30-34	6.70	C	M	R	.	R	C	R	.	C	R	C	.	.	R	.	R	.	.	.	.		late Pleistocene
1H-5, 40-44	8.30	C	M	.	.	F	F	.	.	F	R	F	.	.	.	.	.	.	.	.	.		late Pleistocene
1H-6, 15-19	9.55	A	M	R	.	F	C	.	.	C	.	A	.	.	.	R	.	.	R	.	.		late Pleistocene
1H-7, 3-7	10.93	C	P	.	.	R	F	.	.	R	.	C	.	.	.	.	.	.	.	.	.		late Pleistocene
2H-1, 41-43	11.81	C	M	.	.	F	C	.	.	C	F	C	.	.	.	.	.	.	.	.	.		late Pleistocene
2H-1, 52-54	11.92	C	M	.	.	F	C	.	.	C	.	C	.	.	.	R	.	.	.	.	.		late Pleistocene
2H-1, 101-103	12.41	C	P	.	.	.	C	R	.	F	R	C	R	.	.	R	.	.	.	.	.		late Pleistocene
2H-2, 13-15	13.03	C	M	R	.	F	F	.	.	C	F	C	.	R	.	R	.		.	.	.	*Emiliania huxleyi* Acme	late Pleistocene
2H-2, 51-53	13.41	C	M	.	.	.	F	.	.	C	.	C	.	.	.	.	.	.	.	.	.	*Emiliania huxleyi* Acme	late Pleistocene
2H-2, 125-127	14.15	C	M	.	.	.	F	.	.	C	R	C	.	.	.	.	.	.	.	.	.	*Emiliania huxleyi* Acme	late Pleistocene
2H-3, 41-43	14.81	F	M	R	.	.	F	.	.	F	R	F	.	.	.	.	.	.	.	R	.	*Emiliania huxleyi* Acme	late Pleistocene
2H-3, 52-54	14.92	C	M	.	.	.	C	.	.	C	.	C	.	.	.	.	.	.	.	.	.	*Emiliania huxleyi* Acme	late Pleistocene
2H-3, 120-122	15.60	A	M	.	R	.	C	.	.	C	.	A	.	R	.	.	.	.	.	.	.	*Emiliania huxleyi* Acme	late Pleistocene
2H-4, 5-7	15.95	C	P	.	.	.	C	.	.	R	.	C	.	R	.	.	.	.	.	.	.	*Emiliania huxleyi* Acme	late Pleistocene
2H-4, 61-63	16.51	C	P	.	.	R	C	.	.	F	.	C	.	.	.	.	.	.	.	.	.	*Emiliania huxleyi* Acme	late Pleistocene
2H-5, 19-21	17.59	A	M	.	F	.	C	.	R	C	R	C	.	.	R	R	.	.	.	.	.	*Emiliania huxleyi* Acme	late Pleistocene
2H-5, 22	17.63	A	M	R	F	.	C	.	.	C	.	A	.	.	.	R	.	.	.	.	F	NN21	late Pleistocene
2H-5, 28	17.69	A	M	.	F	.	C	.	.	F	.	A	.	.	.	.	.	.	.	.	F	NN21	late Pleistocene
2H-5, 31	17.72	A	M	.	F	.	C	.	.	F	R	A	.	.	.	.	.	.	.	.	F	NN21	late Pleistocene
2H-5, 59-61	17.99	A	P	.	F	.	C	.	.	F	.	A	.	.	.	.	.	.	.	.	F	NN21	late Pleistocene
2H-5, 62	17.80	A	M	.	F	R	C	.	.	F	.	A	F	R	.	.	.	.	.	.	F	NN21	late Pleistocene
2H-5, 80-84	17.98	C	M	.	F	.	R	.	.	F	.	C	.	.	.	.	.	.	.	.	R	NN21	late Pleistocene
2H-6, 4-6	18.94	F	P	.	.	.	F	.	.	F	.	F	.	.	.	.	.	.	.	.	.	NN21	late Pleistocene
2H-6, 52-54	19.42	C	P	.	F	.	C	R	.	R	.	R	.	.	.	.	.	.	.	.	R	NN21	late Pleistocene
2H-7, 41-43	20.81	C	P	.	.	.	F	.	.	F	.	C	.	.	.	.	.	.	.	.	.	NN21	late Pleistocene
4H-1, 16-18	22.06	F	M	.	.	.	R	.	.	F	R	F	.	.	.	.	.	.	.	.	.	NN21	late Pleistocene
4H-1, 84-88	22.74	F	M	.	.	.	.	.	.	F	.	F	.	.	.	.	.	.	.	.	.	NN21	late Pleistocene
4H-1, 99-101	22.89	F	M	.	.	.	R	.	.	F	.	F	F	.	.	.	.	.	.	.	.	NN21	late Pleistocene
4H-2, 31-33	23.71	F	M	.	R	.	.	.	.	F	.	F	F	.	.	.	.	.	.	.	.	NN21	late Pleistocene
4H-2, 96-100	24.36	R	P	.	.	.	.	.	.	.	.	R	.	.	.	.	.	.	.	.	.	NN21	late Pleistocene
4H-2, 99-101	24.39	F	P	.	R	.	.	.	.	R	.	F	F	R	.	.	.	.	.	.	.	NN21	late Pleistocene
4H-3, 41-43	25.31	F	M	.	.	.	R	.	.	F	.	F	.	.	.	.	.	.	.	.	.	NN21	late Pleistocene
4H-3, 94-96	25.84	F	M	.	.	.	R	.	.	F	.	F	.	R	.	.	.	R	.	.	.	NN21	late Pleistocene
4H-4, 32-34	26.72	F	M	.	.	.	R	.	.	F	.	F	.	.	.	.	.	.	.	.	.	NN21	late Pleistocene
4H-4, 94-96	27.34	F	M	.	.	.	R	.	.	F	.	F	.	.	.	.	.	.	.	.	.	NN21	late Pleistocene
4H-4, 106-108	27.46	F	P	.	.	.	R	.	.	R	.	F	.	.	.	.	.	.	.	R	.	NN21	late Pleistocene
4H-5, 94-98	28.84	C	M	.	R	.	R	.	R	F	R	C	.	.	.	.	.	R	.	.	.	NN21	late Pleistocene
4H-5, 123-125	29.13	C	M	.	.	.	R	.	.	F	R	C	.	.	.	.	.	R	.	.	.	NN21	late Pleistocene
4H-6, 83-85	30.23	C	M	.	R	.	F	.	R	F	.	C	.	R	.	.	.	.	.	.	.	NN21	late Pleistocene
4H-6, 122-126	30.62	C	M	R	F	R	F	R	.	F	R	C	.	R	.	.	.	.	.	.	.	NN21	late Pleistocene
4H-7, 21-25	31.11	C	M	.	.	.	R	R	.	F	R	C	F	R	.	R	.	.	.	.	.	NN21	late Pleistocene
5H-1, 92-96	32.32	F	M	.	.	.	R	.	.	F	R	F	F	R	.	.	.	R	.	.	.	NN21	late Pleistocene

the greater the distance, the shallower the gradient (as in Hole 857C). At Site 855, the depths of the first stratigraphic occurrence of *Emiliania huxleyi* in the three holes is apparently not the first evolutionary occurrence of this species; we believe the holes were not drilled deep enough to reach that datum. The greatest distance between the two datums in question occurs in Hole 857C. This suggests that hydrothermal discharges occurred much deeper here and did not permeate as much of the section. The hydrothermal fluids at this location were probably diverted laterally at depth and discharged in nearby vent fields.

In summary, the nannofossils recorded either earlier or current hydrothermal activity, and in general their state of preservation indicates the intensity of that activity (Fig. 2). The higher the thermal temperature at

Table 7 (continued).

	7		5H-2, 68-72	33.58	F	M	.	.	R	R	.	R	F	R	F	.	R	.	.	.	.	.	.	.		
60			5H-3, 111-115	35.51	C	M	.	.	.	R	.	.	F	.	R	.	.	.	.	.	.	.	.	.		
			5H-4, 9-13	35.99	C	M	.	.	.	R	.	.	F	.	C	.	.	.	.	.	.	.	.	.		
			5H-4, 121-125	37.11	F	P	.	R	.	R	.	.	R	.	R	F	.	.	.	.	.	.	.	.		
	8		5H-5, 79-83	38.19	R	P	.	R	.	R	.	.	.	.	.	R	.	.	.	.	.	.	.	.		
			5H-6, 96-100	39.86	F	VP	.	.	.	.	.	.	.	.	.	F	.	.	.	.	.	.	.	.		
			5H-7, 4-8	40.44	A	M	F	.	.	F	.	.	F	.	A	R	.	.	R	.	.	.	.	.		
			6H-1, 12-16	41.02	C	P	R	.	.	F	.	.	R	.	C	.	.	.	.	.	.	.	.	.		
			6H-2, 5-9	42.45	A	P	R	.	R	F	.	F	R	.	A	C	.	.	.	.	.	.	.	.		
			6H-3, 7-11	43.97	C	M	.	.	.	F	R	R	F	.	C	.	.	.	.	.	.	.	.	.		
			6H-4, 3-7	45.43	C	P	F	.	.	F	R	R	R	.	C	F	.	.	.	.	.	.	.	.		
			6H-5, 9-13	46.99	C	P	.	.	.	R	.	R	.	.	C	.	.	.	.	.	.	.	.	.		
	9		6H-6, 4-8	48.44	A	P	F	R	R	F	.	.	.	.	A	F	.	R	.	.	.	.	.	.		
			6H-7, 8-12	49.98	C	P	R	.	.	R	.	.	R	.	C	R	R	.	.	.	.	.	.	.		
			7H-1, 5-9	50.45	A	M	.	.	.	F	.	.	F	R	A	.	R	R	.	.	.	.	.	.		
			7H-2, 7-9	50.79	A	M	R	.	.	F	.	F	F	.	A	.	.	.	.	.	.	.	.	.		
			7H-3, 135-139	53.57	A	M	R	.	.	F	.	.	F	.	A	R	.	.	.	.	.	.	.	.		
80			7H-4, 1-5	53.63	A	P	R	.	.	F	.	.	R	.	A	.	.	.	.	.	.	.	.	.		
			7H-4, 70-74	54.32	C	M	R	.	.	R	.	.	F	R	C	F	R	F	.	.	.	.	.	.		
	10		7H-5, 80-84	55.57	C	P	R	.	.	F	.	R	R	.	C	.	R	.	.	.	.	.	.	.		
			7H-6, 13-17	55.81	C	M	R	.	.	R	.	.	F	R	C	R	.	R	.	.	.	.	.	.		
			7H-7, 6-10	57.13	A	P	R	.	R	C	.	.	R	.	A	F	.	.	.	.	.	.	.	.		
			8H-2, 107-111	62.47	C	P	.	.	R	F	.	R	R	.	C	R	.	R	.	.	.		.	.	NN21	late Pleistocene
			8H-3, 113-117	64.03	A	P	R	.	.	F	.	.	R	.	A	F	.	.	.	.	.	.	.	.		
			8H-4, 96-100	65.36	C	P	.	.	.	F	.	.	.	.	C	.	.	.	.	.	.	.	.	.		
	11		8H-5, 57-61	66.47	C	P	.	.	.	F	.	R	R	.	C	F	.	.	.	.	.	.	.	.		
			8H-6, 67-71	68.07	C	P	.	.	.	F	.	.	.	.	C	R	.	.	.	.	.	.	.	.		
			8H-7, 64-68	69.54	C	M	R	.	.	F	.	R	F	.	C	F	.	R	R	.	.	.	.	.		
			9H-2, 7-9	70.97	F	M	.	.	.	R	.	.	.	.	F	.	.	.	.	.	.	.	.	.		
			9H-3, 3-8	72.43	A	M	.	.	.	F	.	.	F	R	A	F	.	.	.	.	.	.	.	.		
			9H-4, 3-7	73.93	C	M	.	.	.	F	.	R	R	R	C	F	.	R	.	.	.	.	.	.		
	12		9H-5, 33-38	75.73	C	P	.	.	.	F	.	.	.	.	C	C	.	.	.	.	.	.	.	.		
			9H-5, 79-83	76.19	C	P	.	.	.	F	R	.	.	.	C	F	.	.	.	.	.	.	.	.		
100			9H-6, 41-45	77.31	F	P	.	.	.	F	.	.	.	.	F	R	.	.	.	R	.	.	.	.		
			9H-7, 24-29	78.64	R	M	.	.	.	R	.	.	.	.	.	.	.	.	.	.	.	.	.	.		
			10H-1, 129-131	80.19	C	P	.	.	.	F	.	.	.	.	C	F	.	.	.	.	.	.	.	.		
			10H-2, 138-140	81.78	F	P	.	.	.	R	.	R	.	.	F	F	.	.	.	.	.	.	.	.		
			10H-3, 125-127	83.15	C	P	.	.	R	F	.	.	.	.	C	C	.	.	.	.	.	.	.	.		
	13		10H-4, 117-119	84.57	C	P	.	.	.	F	.	.	R	.	C	F	.	.	.	.	.	.	.	.		
			10H-5, 7-9	84.97	C	P	.	.	.	F	.	.	.	.	C	F	.	.	.	.	.	.	R	.		
			12H-2, 6-8	91.96	C	P	.	.	R	F	.	.	R	.	C	C	.	.	.	.	.	.	.	.		
			13H-1, 49-52	101.99	F	M	.	.	.	R	.	.	R	.	F	R	.	.	.	.	.	.	.	.		
			13H-2, 52-56	103.52	R	P	.	.	.	R	.	.	.	.	R	R	.	.	.	.	.	.	.	.		
	14		13H-4, 107-108	107.07	F	P	.	.	.	F	.	.	.	.	F	R	.	.	.	.	.	.	.	.		

the various sites, the more intense the activity and the poorer the fossil preservation. Because this is an irreversible process, we can detect past hydrothermal activity by investigating nannofossil preservation.

There is also a selective dissolution of individual taxa in response to the hydrothermal activity, which functions much like that caused by dissolution at depth in the oceans near the CCD. Among the placoliths, *Emiliania huxleyi* is less resistant to thermal and fluid corrosion in comparison to *Coccolithus pelagicus,* possibly due to its delicate "T"-shaped elements (Plate 4, Figs. 3, 5, 7, and 10). It disappears in some holes at shallow sub-bottom depths. For example, it disappears abruptly where its abundance is common in Hole 858B (Figure 2); there the heat flow is high (a temperature of 197°C was measured with the WSTP at 19.5 mbsf [see Davis, Mottl, Fisher, et al., 1992]). The more widespread occurrence of *Gephyrocapsa* at relatively deeper sub-bottom depths (e.g., Sample 139-857C-30R-3, 85–88 cm, 316.95 mbsf) and from sediments suffering relatively high temperatures (e.g., Sample 139-856A-6R-1, 44–48 cm, with an estimated temperature lower than 120°C [see Mao et al., this volume]) suggests that *Gephyrocapsa* is more resistant to hydrothermal activity than *Emiliania.*

In *Gephyrocapsa* the loss of the central bridge is sometimes the first stage of dissolution caused by corrosion or thermal alteration (Plate 2, Figs. 5, 6, 8, and 9; Plate 3, Figs. 1, 2, and 3). If hydrothermal activity intensifies, the elements that form the two shields are dissolved bit by bit and separated from each other (Plate 2, Figs. 1, 2, 4, and 7). In some cases, these elements may be heavily corroded and overgrown to form two reinforced shields (Plate 2, Fig. 8). An extreme situation is noted deep in Hole 855C, where spike-like overgrowths project from the outer ends of the elements of both shields (Plate 2, Fig. 9); whether or not these are calcite overgrowths has not been determined.

Coccolithus pelagicus is apparently the most resistant taxon to hydrothermal activity, as evidenced by its occurrences at the deepest depths (e.g., Sample 139-857C-44R-2, 105–109 cm, 392.23 mbsf) and in zones that experienced high temperatures (e.g., the deepest samples from Holes 856A and 858B; Tables 6 and 10). During the initial stages

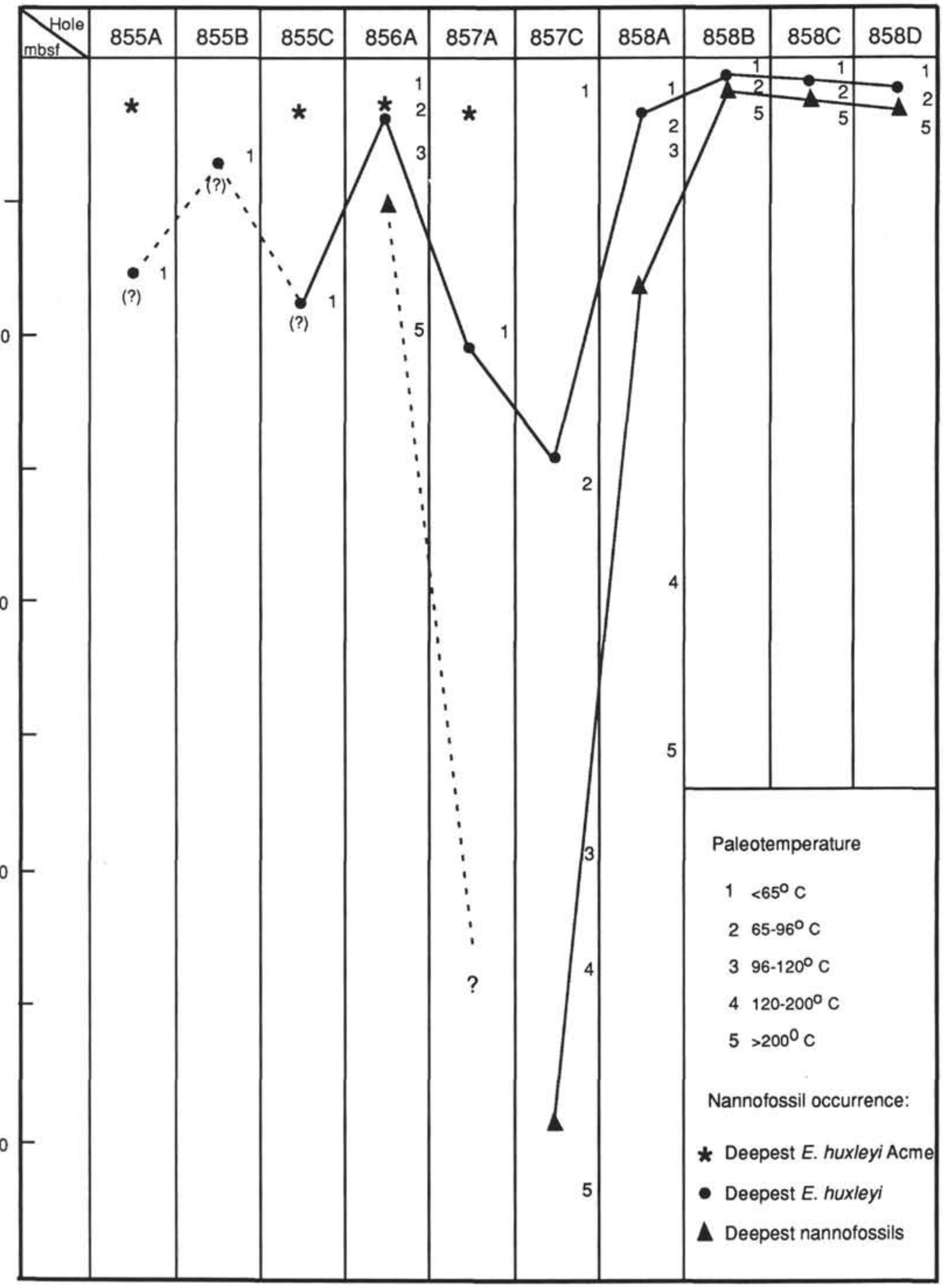

Figure 2. Sub-bottom depths at which the deepest (first) calcareous nannofossils (solid triangles), *Emiliania huxleyi* (solid circles), and *E. huxleyi* Acme (asterisks) occur in Leg 139 holes. Paleotemperatures given in the figure are from Mao et al. (this volume).

of dissolution, the laths forming the two shields of *C. pelagicus* may be partially dissolved (Plate 1, Fig. 9), then subsequently have calcite reprecipitated (Plate 3, Figs. 8, 9; Plate 4, Fig. 1). Ultimately, the coccolith may be transformed into two integrated shields in which individual laths are strongly obscured (Plate 4, Fig. 9). As in the case of *Gephyrocapsa* noted previously, only the wavy or rugged edge of the shield may remain visible to suggest the identity of the taxon.

As noted by Wise (1973), the proximal shield elements of *Coccolithus* are the most susceptible to dissolution, often leaving only the distal shield preserved (Plate 1, Fig. 6). *Calcidiscus leptoporus* displays a similar dissolution phenomenon (Plate 1, Fig. 5).

The dissolution susceptibility of nannofossils subjected to hydrothermal activity in our study area approximates reasonably well that determined empirically for Recent coccoliths in the tropical and extratropical Pacific Ocean by Roth and Berger (1975). These authors found *Emiliania huxleyi* to be less resistant to dissolution than species of *Gephyrocapsa* or *Coccolithus* except for the minute *Gephyrocapsa ericsonii* in tropical areas. They also found that *Coccolithus pelagi-*

Table 8. Distribution of calcareous nannofossils, Hole 857C, Leg 139.

Lithologic unit	Hole 857C Core, section interval (cm)	Depth (mbsf)	Abundance	Preservation	*Braarudosphaera bigelowii*	*Calcidiscus leptoporus*	*Coccolithus crassipons*	*Coccolithus pelagicus*	*Coccolithus streckerii*	*Emiliania huxleyi*	*Gephyrocapsa* Group 1	*Gephyrocapsa* Group 2	*Gephyrocapsa* Group 3	*Gephyrocapsa* Group 4	*Pontosphaera* sp.	*Reticulofenestra* sp.	Zonation (Martini, 1971)	Age (Based on data from forams and nannos)
	1R-2, 125-129	2.75	C	P	.	.	.	F	.	F	C	F	.	R	.			Holocene
	2R-1, 6-11	56.56	C	P	R	.	R	C	.	R	C	F	.	R	.	.		
	2R-2, 50-53	58.50	C	M	R	.	.	F	.	F	C	.	.	.	.	.		
I	3RR-1, 98-100	67.48	C	P	.	.	R	F	.	R	C	F	.	.	.	.		
	3R-2, 93-95	68.93	C	M	.	.	.	R	.	F	C	R	.	.	.	.		
	3R-3, 47-49	69.97	C	M	.	.	.	R	.	R	C	R	.	.	.	.		
	5R-1, 31-35	82.41	R	VP	.	.	.	.	.	.	R	.	.	.	.	.		
	5R-4, 6-9	82.66	R	VP	.	.	.	R	.	.	.	.	.	.	.	.	NN21	late Pleistocene
	5R-5, 36-38	85.46	R	VP	.	.	.	R	.	.	.	.	.	.	.	.		
	6R-1, 119-121	87.39	F	P	.	.	.	R	.	.	F	F	R	.	.	.		
	6R-2, 94-96	88.64	F	P	.	.	.	F	.	.	R	.	.	.	.	.		
IIA	9R-1, 100-102	115.50	R	P	.	.	.	R	.	.	R	.	.	.	.	.		
	10R-1, 3-5	124.13	R	M	.	.	.	R	.	.	.	.	.	.	.	.		
	11R-1, 12-14	133.92	F	M	.	.	.	R	.	F	F	F	R	.	.	R		
	11R-1, 86-88	134.66	F	P	.	.	.	R	.	R	R	F	.	.	.	R		
	12R-1, 100-103	144.50	F	P	.	.	.	R	.	.	R	.	.	R	.	.		
	12R-2, 63-66	145.63	R	P	.	.	.	.	.	R	R	R	R	.	.	.		
	13R-1, 76-80	153.86	R	M	.	.	.	R	.	.	.	.	.	.	.	.		
	13R-2, 55-57	155.15	R	P	.	.	.	R	.	.	.	.	.	.	R	.		
	13R-3, 36-38	156.46	R	P	.	R	.	R	.	.	.	.	R	.	.	.		
	14R-1, 24-28	163.04	R	P	.	.	.	R	.	.	.	.	.	.	.	.		
	15R-1, 27-29	172.77	R	P	.	.	.	R	.	.	.	.	.	.	.	.		
	15R-2, 29-31	174.29	R	P	.	.	.	R	.	.	.	.	.	.	.	.		
	15R-3, 40-42	175.90	R	P	.	.	.	R	.	.	.	.	.	.	.	.		
	18R-1, 92-96	202.52	R	P	.	.	.	R	.	.	.	.	.	.	.	.		
	21R-2, 87-89	232.97	R	P	.	.	.	R	.	.	.	.	.	.	.	.		
	26R-1, 60-62	275.10	R	P	.	.	.	R	.	.	.	.	.	.	.	.		
	28R-1, 112-114	294.92	R	P	.	.	.	R	.	.	.	.	.	.	.	.		
IIB	28R-2, 16-18	295.46	R	P	.	.	.	R	.	.	.	.	.	.	.	.		
	28R-3, 19-22	296.99	R	P	.	.	.	R	.	.	.	.	.	.	.	.		
	29R-1, 45-49	303.85	R	P	.	.	.	R	.	.	.	.	.	.	.	.		
	30R-3, 7-9	316.17	F	VP	.	.	.	F	.	.	R	.	.	.	.	.		
	30R-3, 60-63	316.70	R	P	.	.	.	R	.	.	.	.	.	.	.	.		
	33R-2, 63-65	329.83	R	P	.	.	.	R	.	.	.	.	.	.	.	.	?	?
	34R-1, 71-74	337.21	R	P	.	.	.	R	.	.	.	.	.	.	.	.		
	37R-1, 49-53	351.29	F	P	.	.	.	F	.	.	.	.	.	.	.	.		
	37R-3, 25-29	354.05	R	P	.	.	.	R	.	.	.	.	.	.	.	.		
	38R-1, 111-115	356.91	R	P	.	.	.	R	.	.	.	.	.	.	.	.		
	39R-1, 18-20	360.58	R	P	.	.	.	R	.	.	.	.	.	.	.	.		
	39R-2, 46-48	362.36	R	P	.	.	.	R	.	.	.	.	.	.	.	.		
	39R-3, 80-82	364.20	R	P	.	.	.	R	.	.	.	.	.	.	.	.		
	40R-1, 21-24	365.61	F	P	.	.	.	F	.	.	.	.	.	.	.	.		
	40R-1, 36-39	365.76	F	P	.	.	.	F	.	.	.	.	.	.	.	.		
	40R-2, 68-72	367.58	R	P	.	.	.	R	.	.	.	.	.	.	.	.		
	41R-1, 62-66	375.52	F	P	.	.	.	F	.	.	.	.	.	.	.	.		
	41R-2, 103-106	377.43	R	P	.	.	.	R	.	.	.	.	.	.	.	.		
	41R-3, 57-60	378.47	R	P	.	.	.	R	.	.	.	.	.	.	.	.		
	42R-1, 36-40	380.06	R	P	.	.	.	R	.	.	.	.	.	.	.	.		
	42R-2, 34-37	381.54	R	P	.	.	.	R	.	.	.	.	.	.	.	.		
	43R-2, 23-26	386.43	R	P	.	.	.	R	.	.	.	.	.	.	.	.		
	44R-2, 105-109	392.23	R	P	.	.	.	R	.	.	.	.	.	.	.	.		

cus was more resistant to dissolution than the cool-water tolerant *Gephyrocapsa,* which are the dominant forms found in our study area.

Mixed assemblages that display different states of preservation are quite common in our study area, perhaps due to redeposition of nannofossils from shallow environments along with fine-grained clastic turbidites, which constitute one of the dominant lithologies in the study area. Without this complication, we would have expected to detect a more systematic ranking of hydrothermal alterations among the nannofossil assemblages. In general, however, the preservational state of the nannofossils, if used in conjunction with other methods of paleothermometry, can still be used as a tracer of hydrothermal history.

SUMMARY

Upper Quaternary calcareous nannofossils have been investigated from Leg 139 drill cores from the heavily sedimented Middle Valley of the northern Juan de Fuca Ridge in the northeast Pacific Ocean. The host sediments have been subjected at depth to high temperatures and

Table 9. Distribution of calcareous nannofossils, Hole 858A, Leg 139.

(mbsf)	Core	Lithologic unit	Hole 858A Core, section interval (cm)	Depth (mbsf)	Abundance	Preservation	*Braarudosphaera bigelowii*	*Calcidiscus leptoporus*	*Coccolithus crassipons*	*Coccolithus pelagicus*	*Coccolithus streckerii*	*Emiliania huxleyi*	*Emiliania pujosae*	*Gephyrocapsa* Group 1	*Gephyrocapsa* Group 2	*Gephyrocapsa* Group 3	*Gephyrocapsa* Group 4	*Pontosphaera* sp.	*Reticulofenestra* sp.	*Umbelosphaera tenuis*	Zonation (Martini, 1971)	Age (Based on data from forams. and nannos.)
0	1		1H-1, 93-95	0.93	A	M	R	.	.	C	.	C	.	C	.	.	R	.	.	.		Holocene
			2H-1, 42-44	2.82	R	M	.	.	.	R	.	.	.	R	.	.	.	.	.	.		
	2		2H-2, 19-21	4.09	C	M	.	.	.	C	.	C	R	C	R	.	R	.	.	.		
			2H-5, 6-10	8.46	C	M	R	.	.	F	.	C	R	F	R	.	.	.	.	.		
		I	2H-6, 23-27	10.13	R	P	.	.	.	R	.	.	.	.	.	.	.	.	.	.	NN21	late Pleistocene
			3H-2, 35-37	13.52	R	P	.	R	.	R	.	R	.	.	R	.	.	.	.	.		
	3		3H-3, 44-48	15.11	C	M	.	R	.	R	.	F	R	F	R	.	.	.	.	.		
			3H-4, 68-72	16.85	R	P	.	.	.	R	.	.	.	.	R	.	.	.	.	.		
20			3H-5, 46-50	18.13	R	P	.	.	.	.	.	.	.	.	R	.	.	.	.	.		
			3H-6, 107-111	20.24	C	M	.	.	.	F	.	F	F	C	C	.	.	.	.	.		
			4H-1, 46-50	21.86	A	VP	R	F	.	F	.	.	.	A	.	R	.	.	.	.		
	4		4H-2, 42-46	23.32	F	VP	.	R	.	F	.	.	.	F	.	.	.	.	.	.		
		IIA	4H-3, 44-48	24.84	F	VP	.	F	.	F	.	.	.	F	F	.	.	.	.	R		
			4H-4, 35-39	26.25	C	VP	.	F	.	F	.	.	.	C	.	R	.	.	.	.		
			4H-5, 39-43	27.79	C	VP	F	.	.	F	.	.	.	C	.	R	.	R	.	.		
	5		4H-6, 57-61	29.47	F	VP	R	.	.	F	.	.	.	F	.	.	.	.	.	.		
			4H-7, 43-47	30.83	F	VP	.	.	.	F	.	.	.	F	.	.	.	.	.	.		
40			5H-1, 77-82	31.67	F	VP	R	.	.	F	.	.	.	R	.	.	.	.	.	.		
			5H-2, 92-97	33.32	F	VP	.	.	.	R	.	.	.	F	.	.	.	.	.	.		
	6		5H-3, 88-90	34.78	F	VP	.	.	.	R	.	.	.	F	.	.	R	.	.	.		
			5H-4, 86-89	36.26	F	VP	R	.	.	F	.	.	.	.	.	.	.	.	.	.		
			5H-5, 32-35	37.22	F	VP	R	.	.	.	.	.	.	R	.	F	R	.	.	.	NN21 (?)	late Pleistocene (?)
			5H-6, 22-26	38.62	C	VP	F	.	R	C	.	.	.	.	.	.	.	.	.	.		
	7		6H-1, 31-33	40.71	F	VP	R	.	.	F	.	.	.	.	.	.	.	.	.	.		
			6H-2, 17-18	42.07	F	VP	.	.	.	F	.	.	.	.	.	.	.	.	.	.		
			6H-3, 105-107	44.45	F	VP	.	.	.	F	.	.	.	.	.	.	.	.	.	.		
60	8	IIC	7H-1, 69-72	50.59	F	VP	.	.	.	F	.	.	.	F	.	.	R	R	.	.		
			7H-2, 69-72	52.09	R	VP	.	.	.	R	.	.	.	.	.	.	.	.	.	.		
			7H-3, 72-75	53.62	C	VP	.	.	R	C	.	.	.	F	.	.	R	.	.	.		
	9		7H-4, 78-80	55.18	R	VP	.	.	.	R	.	.	.	.	.	.	.	.	.	.		
			7H-5, 81-85	56.71	R	VP	R	.	.	R	.	.	.	R	.	.	R	.	.	.		
			7H-6, 48-52	57.88	C	VP	.	.	R	C	R	.	.	R	.	.	R	.	.	.		
			8H-1, 69-71	59.59	F	VP	.	.	.	F	R	.	.	F	.	.	R	.	.	.		
	11		8H-3, 70-72	62.48	F	VP	.	.	.	R	.	.	.	R	.	.	R	.	.	.		
80			9H-1, 103-105	63.53	R	VP	.	.	.	R	.	.	.	R	.	.	R	.	.	.		
			9H-2, 67-69	64.67	R	VP	.	.	R	R	.	.	.	R	.	.	R	.	R	.		
			9H-3, 68-72	66.18	F	VP	.	.	R	F	.	.	.	F	.	.	R	.	.	.		
	12		9H-4, 57-61	67.57	R	VP	.	.	.	R	.	.	.	R	.	.	R	.	.	.		
			9H-6, 61-65	70.61	F	VP	.	.	R	F	.	.	.	.	.	.	.	.	.	.		
			12H-1, 10-12	81.70	F	VP	.	.	.	F	.	.	.	.	.	.	R	.	.	.		

hot hydrothermal fluids that have altered or destroyed in part or in toto the nannofossil assemblages, thereby raising at several sites the level of the first (deepest) stratigraphic occurrence of nannofossils or of the important *Emiliania huxleyi* datum. The degree of alteration of the nannofossil assemblages is dependent on the intensity of the heat and/or hydrothermal activity, which are indicated by paleotemperatures derived independently from studies of color alteration of palynomorphs and by vitrinite reflectance (Mao et al., this volume). State of preservation and the downhole level at which assemblages have been destroyed correlate well with the inferred paleotemperature estimates. Destruction of the assemblages appears to be species selective, and follows in general the dissolution rankings determined independently by others for Recent nannofossils of the Pacific basin. More systematic correlation of these phenomena are hampered, however, by the fact that nannofossil preservation is already quite variable at the time of deposition because of the predominance of turbidite activity in the study area.

ACKNOWLEDGMENTS

We thank Drs. Eric de Kaenel and Wuchang Wei for reviewing critical slides, for their helpful discussion, and for their reviews of the

Table 10. Distribution of calcareous nannofossils, Holes 858B, 858C, and 858D, Leg 139.

Hole	Core	Lithologic unit	Core, section interval (cm)	Depth (mbsf)	Abundance	Preservation	*Braarudosphaera bigelowii*	*Calcidiscus leptoporus*	*Coccolithus crassipons*	*Coccolithus pelagicus*	*Coccolithus streckerii*	*Emiliania huxleyi*	*Emiliania pujosae*	*Gephyrocapsa* Group 1	*Gephyrocapsa* Group 2	*Gephyrocapsa* Group 3	*Gephyrocapsa* Group 4	*Pontosphaera japonica*	*Pontosphaera* sp.	*Reticulofenestra* sp.	*Umbelosphaera tenuis*	Zonation (Martini, 1971)
858B	1	I	1H-1, 84-88	0.84	R	P	.	R	.	R	.	.	.	R	.	.	R	.	.	.	R	NN21
			1H-2, 68-72	2.18	C	M	.	.	.	C	.	C	.	C	.	.	R	.	.	.	.	
			1H-3, 58-62	3.58	A	M	.	.	R	C	R	C	F	C	.	.	R	.	R	.	.	
			1H-4, 60-64	5.10	R	M	.	.	.	R	.	.	.	.	.	.	R	.	.	.	.	
			1H-5, 45-47	6.45	C	VP	.	.	.	C	.	.	.	.	.	.	.	.	.	.	.	
858C	1	I	1H-1, 66-70	0.66	F	M	.	.	.	R	.	F	.	F	.	.	R	.	.	.	.	NN21
			1H-2, 52-56	2.02	C	M	R	.	R	C	F	C	.	C	.	.	R	R	.	.	.	
			1H-3, 25-29	3.25	A	M	.	.	.	C	R	C	.	C	.	.	F	F	.	R	.	
	2		2H-2, 88-90	5.88	C	M	.	.	.	C	R	C	F	C	R	.	R	.	.	.	.	
			2H-3, 29-31	6.79	C	P	.	.	R	C	R	.	.	F	F	.	.	.	.	.	.	
			2H-4, 44-46	8.44	C	P	.	.	.	C	R	R	.	C	F	R	R	.	.	.	.	
			2H-5, 39-41	9.89	C	VP	.	.	.	C	.	F	.	C	F	.	R	.	.	.	.	
			2H-6, 68-70	11.68	F	VP	.	.	.	F	.	R	.	R	.	.	R	.	.	.	.	
858D	1	I	1H-1, 0-1	0.77	R	P	.	R	.	.	.	R	.	R	.	.	R	.	.	.	.	NN21
			1H-1, 77-81	0.77	C	P	.	.	.	C	.	F	.	C	F	.	R	.	.	.	.	
			1H-2, 84-88	2.34	C	P	.	.	.	F	.	R	R	C	F	.	R	.	.	.	.	
			1H-3, 52-56	3.52	R	VP	.	.	.	R	.	.	.	R	.	.	.	.	.	.	.	
			1H-4, 64-65	5.11	A	M	.	.	R	C	.	C	.	C	.	.	R	.	.	.	.	
			1H-5, 68-72	6.68	C	P	.	.	.	F	.	F	R	C	R	.	R	.	.	.	.	
			1H-6, 86-90	8.36	F	P	.	.	.	F	.	.	.	.	.	.	.	.	.	.	.	NN21 (?)
			1H-CC	9.30	R	P	.	R	.	R	.	.	.	R	.	.	.	.	.	.	.	
	2		2H-1, 58-61	9.88	F	P	.	.	.	F	.	.	.	R	.	.	R	.	.	.	.	
			2H-2, 103-105	11.83	R	P	.	.	.	R	.	.	.	.	.	.	.	.	.	.	.	
			2H-CC	18.80	F	VP	.	.	.	F	.	.	.	R	.	.	R	.	.	.	.	

manuscript. Smear slides were made by Ms. Xinlan Liu, Li Liu, and Kimberley Hall; Li Liu also helped prepare tables in the text. The SEM was skillfully operated by Ms. Kim Riddle. The study was supported by USSAC funds; NSF grant DPP 91-18480 provided necessary laboratory facilities.

REFERENCES*

Berggren, W.A., Kent, D.V., and Van Couvering, J.A., 1985. The Neogene: Part 2. Neogene geochronology and chronostratigraphy. *In* Snelling, N.J. (Ed.), *The Chronology of the Geological Record.* Geol. Soc. London Mem., 10:211–260.

Bramlette, M.N., 1961. Pelagic sediments. *In* Sears, M. (Ed.), *Oceanography.* Am. Assoc. Adv. Sci. Publ., 67:345–366.

Davis, E.E., Mottl, M.J., Fisher, A.T., et al., 1992. *Proc. ODP, Init. Repts.,* 139: College Station, TX (Ocean Drilling Program).

Gard, G., 1988. Late Quaternary calcareous nannofossil biozonation, chronology and paleo-oceanography in areas north of the Faeroe-Iceland Ridge. *Quat. Sci. Rev.,* 7:65–78.

Gard, G., and Backman, J., 1990. Synthesis of Arctic and Subarctic coccolith biochronology and history of North Atlantic drift water influx during the last 500,000 years. *In* Bleil, U., et al. (Eds.), *Geologic History of the Polar Oceans: Arctic versus Antarctic.* NATO ASI Ser., Ser. C., 417–436.

Gartner, S., 1977. Calcareous nannofossil biostratigraphy and revised zonation of the Pleistocene. *Mar. Micropaleontol.,* 2:1–25.

Martini, E., 1971. Standard Tertiary and Quaternary calcareous nannoplankton zonation. *In* Farinacci, A. (Ed.), *Proc. 2nd Int. Conf. Planktonic Microfossils Roma:* Rome (Ed. Tecnosci.), 2:739–785.

Matsuoka, H., and Okada, H., 1989. Quantitative analysis of Quaternary nannoplankton in the subtropical northwestern Pacific Ocean. *Mar. Micropaleontol.,* 14:97–118.

————, 1990. Time-progressive morphometric changes of the genus *Gephyrocapsa* in the Quaternary sequence of the tropical Indian Ocean. *In* Duncan, R.A., Backman, J., Peterson, L.C., et al., *Proc. ODP, Sci. Results,* 115: College Station, TX (Ocean Drilling Program), 255–270.

McIntyre, A., and McIntyre, R., 1971. Coccolith concentrations and differential solution in oceanic sediments. *In* Funnel, B.M., and Riedel, W.R. (Eds.), *The Micropaleontology of Oceans:* London (Cambridge Univ. Press), 253–261.

* Abbreviations for names of organizations and publications in ODP reference lists follow the style given in *Chemical Abstracts Service Source Index* (published by American Chemical Society).

Perch-Nielsen, K., 1985. Cenozoic calcareous nannofossils. *In* Bolli, H.M., Saunders, J.B., and Perch-Nielsen, K. (Eds.), *Plankton Stratigraphy:* Cambridge (Cambridge Univ. Press), 427–554.

Rio, D., 1982. The fossil distribution of coccolithophore genus *Gephyrocapsa* Kamptner and related Plio-Pleistocene chronostratigraphic problems. *In* Prell, W.L., Gardner, J.V., et al., *Init. Repts. DSDP,* 68: Washington (U.S. Govt. Printing Office), 325–343.

Rio, D., Raffi, I., and Villa, G., 1990. Pliocene-Pleistocene calcareous nannofossil distribution patterns in the Western Mediterranean. *In* Kastens, K.A., Mascle, J., et al., *Proc. ODP, Sci. Results,* 107: College Station, TX (Ocean Drilling Program), 513–533.

Roth, P.H., and Berger, W.H., 1975. Distribution and dissolution of coccoliths in the south and central Pacific. *In* Sliter, W.V., Bé, A.W.H., and Berger, W.H. (Eds.), *Dissolution of Deep-Sea Carbonates.* Spec. Publ. Cushman Found. Foraminiferal Res., 13:87–113.

Sato, T., Kameo, K., and Takayama, T., 1991. Coccolith biostratigraphy of the Arabian Sea. *In* Prell, W.L., Niitsuma, N., et al., *Proc. ODP, Sci. Results,* 117: College Station, TX (Ocean Drilling Program), 37–54.

Schneidermann, N., 1977. Selective dissolution of Recent coccoliths in the Atlantic Ocean. *In* Ramsay, A.T.S. (Ed.), *Oceanic Micropaleontology:* New York (Academic Press), 1009–1053.

Spaulding, S., 1991. Neogene nannofossil biostratigraphy of Sites 723 through 730, Oman Continental Margin, northwestern Arabian Sea. *In* Prell, W.L., Niitsuma, N., et al., *Proc. ODP, Sci. Results,* 117: College Station, TX (Ocean Drilling Program), 5–36.

Takayama, T., and Sato, T., 1987. Coccolith biostratigraphy of the North Atlantic Ocean, Deep Sea Drilling Project Leg 94. *In* Ruddiman, W.F., Kidd, R.B., Thomas, E., et al., *Init. Repts. DSDP,* 94 (Pt. 2): Washington (U.S. Govt. Printing Office), 651–702.

Turekian, K.K., 1965. Some aspects of the geochemistry of marine sediments. *In* Riley, J.P., and Skirrow, G. (Eds.), *Chemical Oceanography:* New York (Academic Press), 2:81–126.

Verbeek, J.W., 1990. Late Quaternary calcareous nannoplankton biostratigraphy for the Northern Atlantic Ocean. *Meded. Rijks Geol. Dienst,* 44:14–33.

Wise, S.W., Jr., 1973. Calcareous nannofossils from cores recovered during Leg 18, Deep Sea Drilling Project: biostratigraphy and observations of diagenesis. *In* Kulm, L.D., von Huene, R., et al., *Init. Repts. DSDP,* 18: Washington (U.S. Govt. Printing Office), 569–615.

————, 1977. Chalk formation: early diagenesis. *In* Anderson, N.R., and Malahoff, A. (Eds.), *The Fate of Fossil Fuel CO_2 in the Oceans:* New York (Plenum), 717–739.

Date of initial receipt: 29 March 1993
Date of acceptance: 22 October 1993
Ms 139SR-208

APPENDIX

Calcareous nannofossils encountered in alphabetical order of generic epithets (for bibliographic references, see Perch-Nielsen, 1985).

Braarudosphaera bigelowii (Gran and Braarud, 1935) Deflandre, 1947
Calcidiscus leptoporus (Murray and Blackman, 1898) Loeblich and Tappan, 1978
Coccolithus crassipons Bouché, 1962
Coccolithus pelagicus (Wallich, 1877) Schiller, 1930
Coccolithus streckerii Takayama and Sato, 1987
Crenalithus doronicoides (Black and Barnes, 1961) Roth, 1973
Emiliania huxleyi (Lohmann, 1902) Hay and Mohler *in* Hay et al., 1967
Emiliania pujosae Verbeek, 1990
Gephyrocapsa Group 1, this paper (modified from Gard, 1988)
Gephyrocapsa Group 2, Gard, 1988
Gephyrocapsa Group 3, Gard, 1988
Gephyrocapsa Group 4, this paper
Helicosphaera inversa Gartner, 1980
Helicosphaera kamptneri Hay and Mohler *in* Hay et al., 1967
Helicosphaera wallichii (Lohmann, 1902) Boudreaux and Hay, 1969
Pontosphaera japonica (Takayama, 1967) Nishida, 1971
Pontosphaera sp.
Reticulofenestra sp.
Syracosphaera pulchra Lohmann, 1902
Syracosphaera sp.
Umbellosphaera tenuis (Kamptner, 1937) Paasche *in* Markali and Paasche, 1955

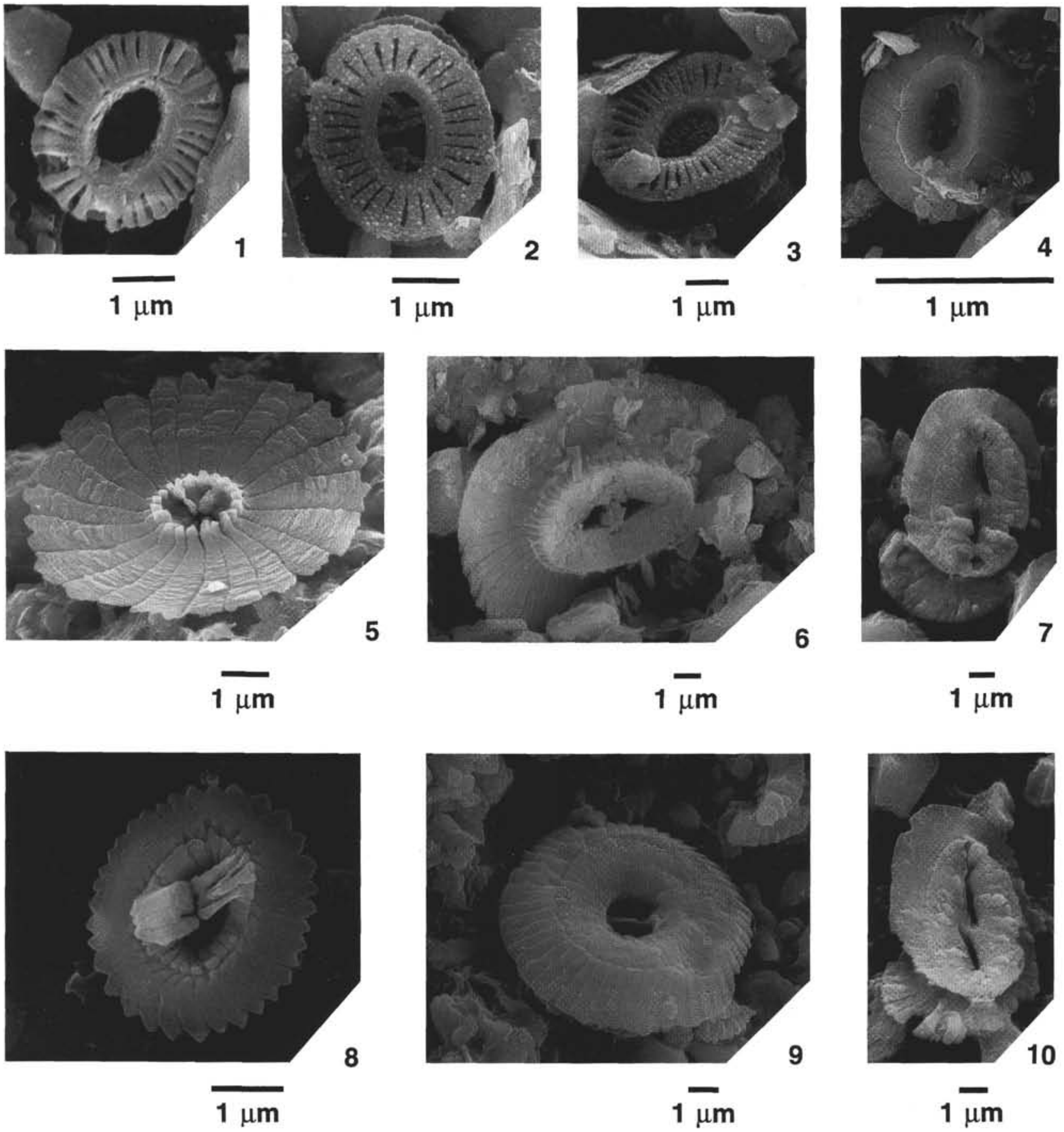

Plate 1. All figures are SEM micrographs. Magnifications are indicated by a bar scale below each figure. **1–2.** *Emiliania huxleyi;* (1) Sample 139-857A-2H-5, 19–21 cm, distal view; (2) Sample 139-855C-2R-6, 84–88 cm, cold water form with solid proximal shield. **3.** *Emiliania pujosae,* Sample 139-855C-2R-6, 84–88 cm. **4.** *Coccolithus* sp., Sample 139-855C-9R-CC, distal view. **5.** *Calcidiscus leptoporus,* Sample 139-856A-7R-3, 18–22 cm, proximal view. **6.** *Coccolithus crassipons,* Sample 139-855C-9R-1, 44–48 cm, proximal view. **7, 10.** *Helicosphaera wallichii,* Sample 139-856A-3H-5, 74–78 cm, proximal views. **8.** *Gephyrocapsa* Group 1, Sample 139-855A-7R-3, 18–32 cm, distal view; corrosion has sharply delineated the three or four lath-shaped elements that form the bridge. **9.** *Coccolithus* sp., Sample 139-855A-1R-1, 94–98 cm, proximal view.

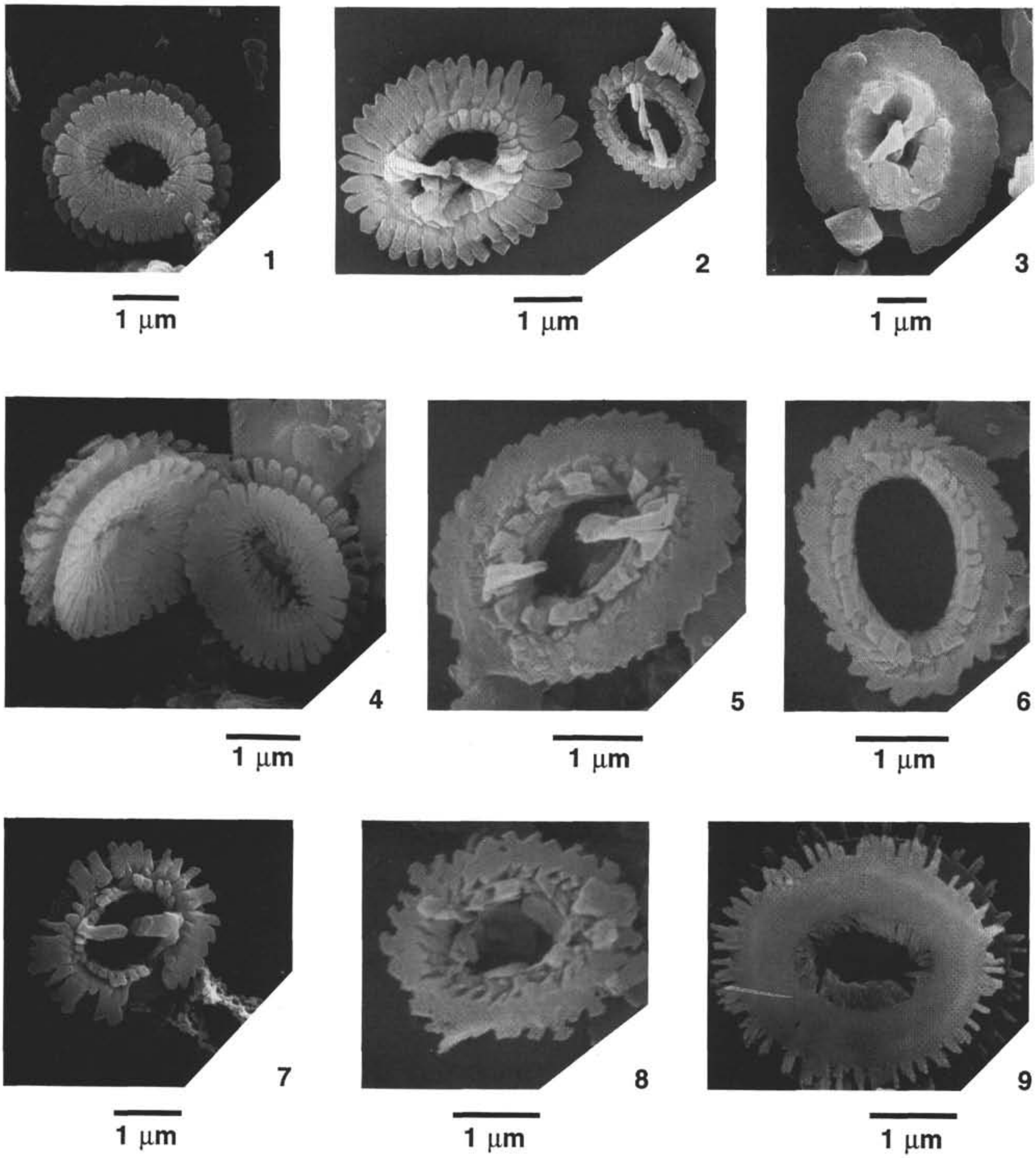

Plate 2. All figures are SEM micrographs. Magnifications are indicated by a bar scale below each figure. **1.** *Gephyrocapsa* sp., specimen slightly dissolved, Sample 139-855A-7R-3, 18–22 cm, proximal view. **2.** *Gephyrocapsa* Group 1 (left) and Group 2 (right), specimens slightly dissolved, Sample 139-855A-7R-3, 18–22 cm, distal views. **3, 5.** *Gephyrocapsa* Group 4, distal views. (3) Sample 139-855C-10R-5, 7–11 cm; (5) Sample 139-855A-1R-4, 94–97 cm. **4.** *Gephyrocapsa* Group 1, specimens slightly dissolved, Sample 139-855C-9R-1, 44–48 cm, oblique proximal views. **6, 8.** *Gephyrocapsa* Group 1, specimens dissolved and overgrown, distal views; (6) Sample 139-855A-1R-4, 94–97 cm; (8) Sample 139-855R-1, 91–94 cm. **7.** *Gephyrocapsa* Group 1, specimen partially dissolved, Sample 139-855A-7R-3, 18–22 cm, distal view. **9.** *Gephyrocapsa* Group 3, altered specimen with spike-like overgrowths of calcite(?) along the edges of both proximal and distal shields, Sample 139-855C-9R-1, 44–48 cm, proximal view.

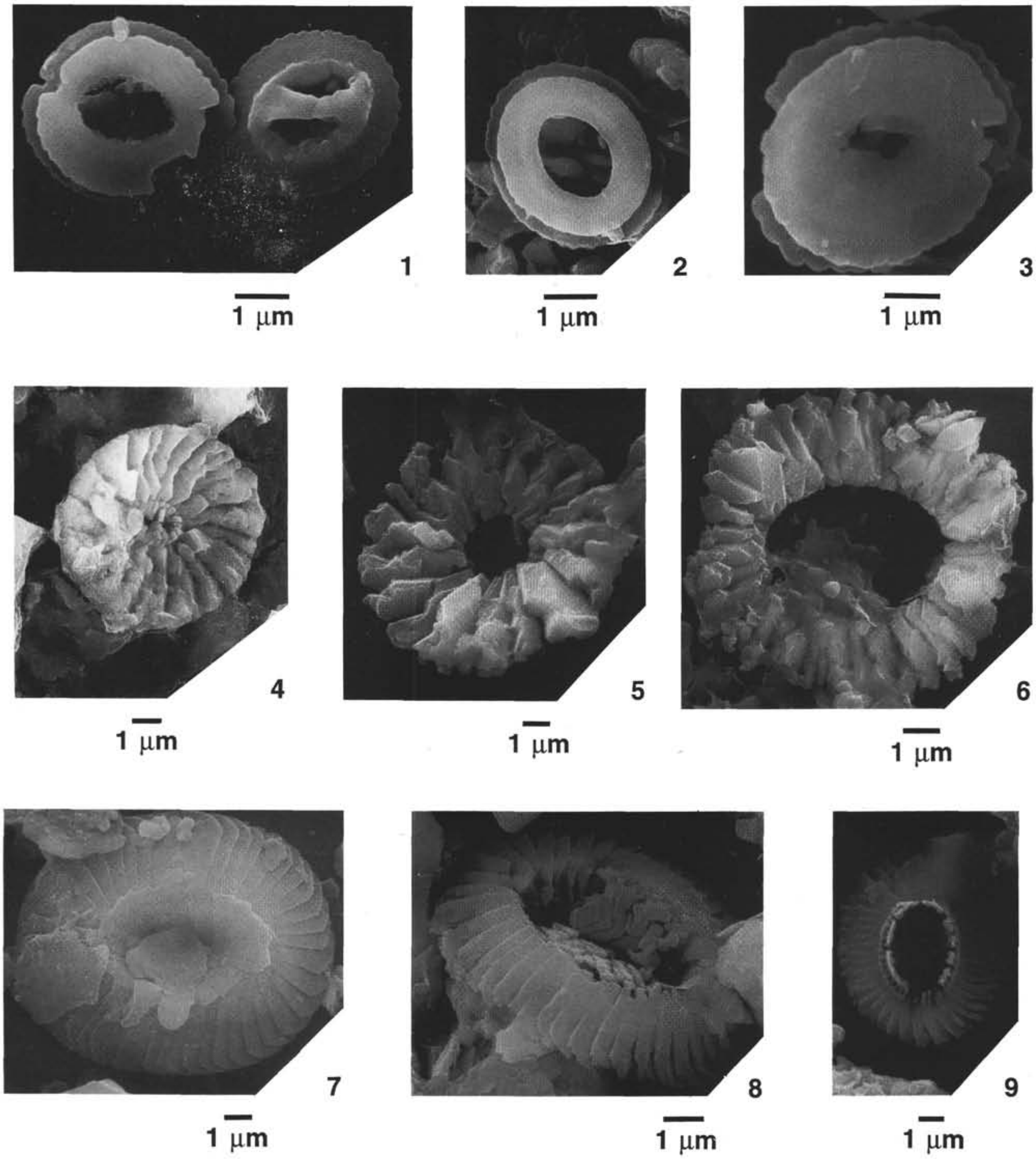

Plate 3. All figures are SEM micrographs. Magnifications are indicated by a bar scale below each figure. **1.** *Gephyrocapsa* Group 4 (left, proximal view) and Group 3 (right, distal view), showing mixed preservation of poor (left) to moderate (right), Sample 139-857A-12X-2, 6–8 cm. **2.** *Gephyrocapsa* Group 4, specimen corroded and missing a central bridge, Sample 139-855C-10R-5, 7–11 cm, proximal view. **3.** *Gephyrocapsa* Group 3, corroded specimen without central bridge, Sample 139-855C-9R-1, 44–48 cm, proximal view. **4–5.** *Calcidiscus leptoporus,* showing mixed preservations of moderate to poor (from left to right), Sample 139-856A-3H-5, 74–78 cm, proximal views. **6–9.** *Coccolithus pelagicus;* (6) poorly preserved distal shield, Sample 139-856A-3H, 74–78 cm; (7) well-preserved specimen, Sample 139-855A-1R-1, 91–94 cm, distal view; (8–9) specimens dissolved and overgrown, distal views, [8] Sample 139-855C-9R-1, 44–48 cm; [9] Sample 139-855C-2R-6, 84–88 cm.

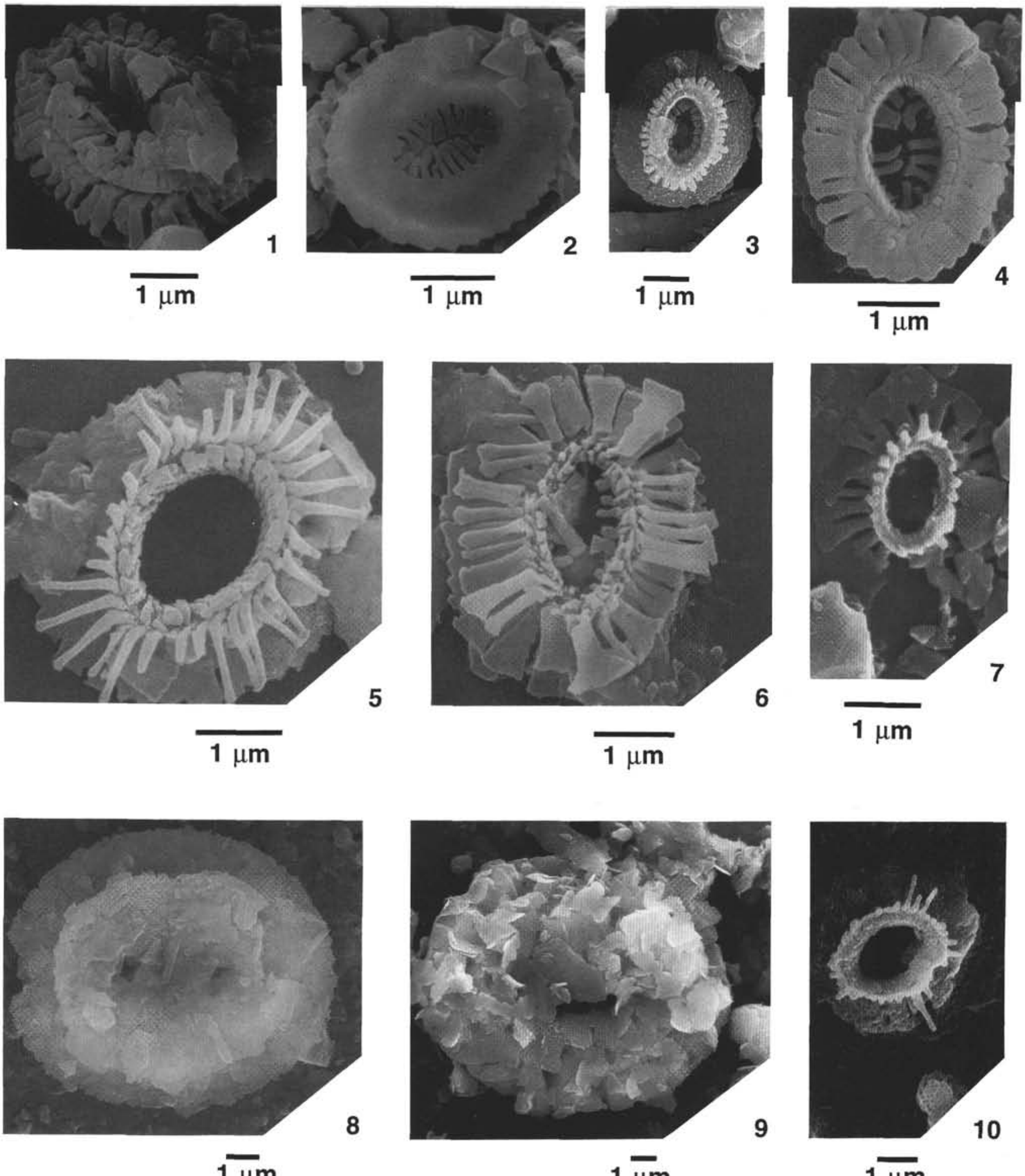

Plate 4. All figures are SEM micrographs. Magnifications are indicated by a bar scale below each figure. **1.** *Gephyrocapsa* sp., specimen strongly dissolved and overgrown, Sample 139-855C-9R-1, 44–48 cm, distal view. **2.** *Emiliania huxleyi,* cold-water form with solid proximal shield, Sample 139-855A-4R-3, 22–24 cm. **3, 7, 10.** *Emiliania huxleyi,* specimens with distal shields partly corroded and dissolved; (3) cold-water form with solid proximal shield, Sample 139-855C-2R-6, 84–88 cm; (7) Sample 139-857A-2H-5, 19–21 cm; (10) cold-water form with solid proximal shield, Sample 139-855A-3H-5, 74–78 cm. **4.** *Emiliania huxleyi,* specimen with heavy overgrowth, Sample 139-856A-1R-4, 94–97 cm. **5, 6.** *Emiliania pujosae*; (5) specimen corroded partly, Sample 139-855A-1R-4, 94–97 cm; (6) specimen corroded with overgrowth, Sample 139-855A-1R-4, 94–97 cm. **8, 9.** *Coccolithus pelagicus*?; (8) specimen dissolved and overgrown, Sample 139-856A-5H-2, 31–39 cm; (9) specimen with poor preservation (with overgrowth after dissolution), Sample 139-856A-5H-2, 31–39 cm.